

12

FG.

RADC-TR-76-118
Final Technical Report
May 1976

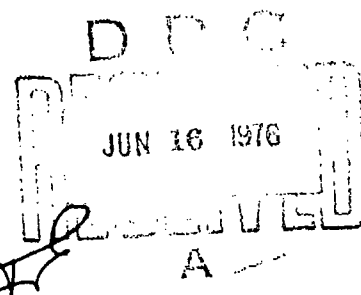


RECTANGULAR PLAT-PACK LIDS UNDER EXTERNAL PRESSURE

Syracuse University

AD A 025 625

Approved for public release;
distribution unlimited.



Rome Air Development Center
Air Force Systems Command
Griffiss Air Force Base, New York 13441

This report has been reviewed by the RADC Information Office (OI) and is releasable to the National Technical Information Service (NTIS). At NTIS it will be releasable to the general public including foreign nations.

This report has been reviewed and is approved for publication.

APPROVED:

Garf. Menlo

PETER F. MANNO
Project Engineer

APPROVED:

Joel Marshy

JOSEPH J. NARESKY
Chief, Reliability and Compatibility Division

FOR THE COMMANDER:

MR: *John P. Huss*
JOHN P. HUSS

JOHN P. HUSS
Acting Chief, Plans Office

ACCESSION for

NTM

UNC

UNC

UNC

61

A

Do not return this copy. Retain or destroy.

UNCLASSIFIED

SECURITY CLASSIFICATION OF THIS PAGE (When Data Entered)

REPORT DOCUMENTATION PAGE		READ INSTRUCTIONS BEFORE COMPLETING FORM	
1. REPORT NUMBER RADC TR-76-118	2. GOVT ACCESSION NO.	3. RECIPIENT'S CATALOG NUMBER	
4. TITLE (and Subtitle) RECTANGULAR FLAT-PACK LIDS UNDER EXTERNAL PRESSURE,	5. TYPE OF REPORT & PERIOD COVERED Final Technical Report, Jun 73 - Sep 74	6. PERFORMING ORG. REPORT NUMBER TR-74-2	
7. AUTHOR(s) Charles Libove	8. CONTRACT OR GRANT NUMBER(s) F30602-71-C-0312	9. PERFORMING ORGANIZATION NAME AND ADDRESS Syracuse University/Dept of Industrial Engineering and Operations Research Syracuse NY 13210	
10. CONTROLLING OFFICE NAME AND ADDRESS Rome Air Development Center (RBRM) Griffiss AFB NY 13441	11. REPORT DATE May 1976	12. NUMBER OF PAGES 62	
13. MONITORING AGENCY NAME & ADDRESS (if different from Controlling Office) Same	14. SECURITY CLASS. (of this report) UNCLASSIFIED	15. DECLASSIFICATION/DOWNGRADING SCHEDULE N/A	
16. DISTRIBUTION STATEMENT (of this Report) Approved for public release; distribution unlimited.			
17. DISTRIBUTION STATEMENT (of the abstract entered in Block 20, if different from Report) Same			
18. SUPPLEMENTARY NOTES RADC Project Engineer: Peter F. Manno (RBRM)			
19. KEY WORDS (Continue on reverse side if necessary and identify by block number) Flat-Packs centrifuge elastic restraint hermeticity bomb pressure plate theory Qualification procedures lid seal tensile stresses reliability Screening tests lid deflection			
20. ABSTRACT (Continue on reverse side if necessary and identify by block number) An analysis is made of the tensile stresses in the lid seal and the lid deflections for a rectangular flat-pack under external pressure. On the basis of this analysis, formulas and charts are presented to facilitate (a) the proper design of the package so that it will retain its hermeticity under a given screening pressure and (b) the selection of the proper pressure to use in the hermeticity screening of an already designed package. (Cont'd)			

DD FORM 1473

1 JAN 73

EDITION OF 1 NOV 65 IS OBSOLETE

UNCLASSIFIED

SECURITY CLASSIFICATION OF THIS PAGE (When Data Entered)

409100

1.1

UNCLASSIFIED

SECURITY CLASSIFICATION OF THIS PAGE(When Data Entered)

Information is also given on the approximate equivalence of external pressure and centrifuge acceleration in regard to the seal stresses and lid deflections of a rectangular flat-pack.

UNCLASSIFIED

SECURITY CLASSIFICATION OF THIS PAGE(When Data Entered)

CONTENTS

	Page
SUMMARY	1
INTRODUCTION	1
ELASTIC RESTRAINT FURNISHED BY WALLS	3
BASIC DATA FROM PLATE THEORY	5
FORMULAS FOR TENSILE STRESS IN THE SEAL	7
APPLICATION TO DESIGN AND SCREENING	9
FLAT-PACKS IN A CENTRIFUGE	13
NUMERICAL EXAMPLES	16
CONCLUDING REMARKS	20
APPENDIX A: SMALL DEFLECTION ANALYSIS OF A UNIFORMLY LOADED ELASTIC RECTANGULAR PLATE WITH EDGES ELASTICALLY RESTRAINED AGAINST ROTATION	24
APPENDIX B: SMALL-DEFLECTION ANALYSIS OF A UNIFORMLY LOADED ELASTIC RECTANGULAR PLATE WITH CLAMPED EDGES	36
APPENDIX C: REMARKS ON THE CORNER STRESS	49
REFERENCES	51
FIGURES	52

EVALUATION

This study was performed in support of the overall program of the Solid State Applications Section directed toward developing adequate reliability screening and qualification testing sequences for micro-electronic devices in accordance with the Reliability Technical Program Objective No. 13. It successfully met its objective which was to provide a means for predicting the stress on the lid seal of a hermetic package under various levels of pressure and constant acceleration. These levels are included in the screening procedures imposed by MIL-M-38510 and MIL-STD-883. The results of the study will be used by the Air Force to establish effective test levels as a function of package size and material and also by part manufacturers as design guidelines. The equations which have been developed will first be verified by experimentation and then used for formulating revised screening requirements in MIL-STD-883A, "Test Methods and Procedures for Microelectronics," in the preparation of proposed Method 5008, "Test Procedures for Hybrid and Multichip Microcircuits" to MIL-STD-883A and in support of the JLC Joint Technical Coordinating Group Subtask on Hybrid Microcircuit Technology Base.

Peter F. Manno

PETER F. MANNO
Solid State Applications Section
Reliability Branch

SUMMARY

4
An analysis is made of the tensile stresses in the lid seal and the lid deflections for a rectangular flat-pack under external pressure. On the basis of this analysis, formulas and charts are presented to facilitate (a) the proper design of the package so that it will retain its hermeticity under a given screening pressure and (b) the selection of the proper pressure to use in the hermeticity screening of an already designed package.

Information is also given on the approximate equivalence of external pressure and centrifuge acceleration in regard to the seal stresses and lid deflections of a rectangular flat-pack.

INTRODUCTION

External pressure, per Method 1014 of reference 1, is generally accepted as a means of screening out non-hermetic or potentially non-hermetic microelectronic packages. Knowing that this is the screening device to be employed, the designer and the user of such packages are then faced with the following two important questions, respectively:

- (a) Given the screening pressure to which the package will be subjected, what should the design features of the package be in order that a seal of good quality will retain its hermeticity under that pressure?
- (b) Given a package that is already designed and available, what screening pressure should be used in order to weed out (i.e., destroy the hermeticity or aggravate the non-hermeticity of) those seals at the low end of the quality spectrum?

This report is intended as an aid in answering these two questions, with particular reference to flat-pack configuration shown in Figure 1.

The following two hypotheses form the main basis of the present work:

- (a) Under external pressure the lid of the package may be regarded as a uniformly loaded rectangular plate with edges elastically restrained against rotation, this restraint being furnished by the walls of the package.
- (b) The external pressure weeds out unsatisfactory seals by creating tensile stresses in the sealing material that exceed the tensile strength of that material. (In poor quality seals (for example, those containing voids or inclusions of foreign matter) this tensile strength will presumably be lower than in good quality seals.)

SYMBOLS

The following symbols will be used for the geometric parameters and elastic constants. Other symbols will be introduced as needed.

- a = width of lid (in.)
- b = length of lid (in.) ($b \geq a$)
- t = thickness of lid (in.)
- w = thickness of walls (in.)
- h = inside height of walls (in.)
- E_c = Young's modulus of lid material (psi)
- E_w = Young's modulus of wall material (psi)
- ν_c = Poisson's ratio of lid material
- ν_w = Poisson's ratio of wall material
- $D_c = E_c t^3 / [12(1 - \nu_c^2)]$ = plate flexural stiffness of lid
- $D_w = E_w w^3 / [12(1 - \nu_w^2)]$ = plate flexural stiffness of walls

ELASTIC RESTRAINT FURNISHED BY WALLS

The walls will be regarded as wide vertical beams of height h , with the local rotation θ (in radians) at the upper end proportional to the local intensity M of the bending moment per unit width exerted upon the wall by the edge of the lid. This relationship can be expressed as

$$M = k\theta \quad (1)$$

where k is a proportionality constant. The value of k depends upon the restraint which the base of the package furnishes to the lower edge of the wall. Two bracketing cases can be envisioned and are illustrated in Figure 2. In one of these (Fig. 2(a)) the base is so stiff in bending (perhaps because of a thick substrate bonded to its entire surface) that it prevents essentially any rotation of the lower edge of the wall. In this case beam theory gives

$$k = 4 D_w/h \quad (2)$$

In the second case (Fig. 2(b)) the base of the package has the same flexural stiffness as the lid and, therefore, with the package under hydrostatic pressure, the lower edge of the wall will be subjected to bending moments of the same magnitude as the upper edge. In that case it can be shown that

$$k = 2 D_w/h \quad (3)$$

The actual state of affairs will lie somewhere between these two, and, therefore, k will be given the following representation:

$$k = \alpha D_w/h \quad (4)$$

where α lies between 4 and 2, with its actual value depending on the flexural stiffness of the base of the package. In the absence of better information a value of α equal to 3 is suggested. It will be seen later that this uncertainty regarding the exact value of α will usually be of very little consequence.

For later use the following non-dimensional measure of k will now be introduced:

$$K \equiv \frac{4}{\pi} \frac{ak}{D_c} = \frac{4}{\pi} (\alpha \frac{D_w}{D_c} \frac{a}{h}) \quad (5)$$

This definition can be rewritten as follows:

$$K \equiv \frac{4}{\pi} K^1 \quad (5a)$$

where

$$K^1 \equiv \alpha \frac{D_w}{D_c} \frac{a}{h} \quad (6)$$

If the Poisson's ratios of the lid and wall materials are the same, the last equation reduces to

$$K^1 \equiv \alpha \frac{E_w}{E_c} \left(\frac{w}{t}\right)^3 \frac{a}{h} \quad (6a)$$

In the graphs to be presented it will be advantageous to show various quantities as functions of $\arctan K$, rather than as functions of K . Therefore, Figure 3 is presented to permit an easy conversion from K to $\arctan K$. In Figure 3 there is also a graph to facilitate the conversion from K^1 to $\arctan K$.

BASIC DATA FROM PLATE THEORY

Under the action of a uniform gage pressure p (psi), reactions will develop along the edges and at the corners of the flat-pack lid, as depicted in Figure 4. These will include bending moments of varying intensity M (in.-lb. per in.) due to the restraint against rotation furnished by the walls, vertical forces of varying intensity V (lb. per in.), and concentrated downward forces of magnitude R (lb.), due to the tendency of the corners to rise. The maximum values of M and V occur at the middle of the long side. These, together with R , can be expressed as

$$M_{\max} = n_1 \cdot pa^2 \quad (7)$$

$$V_{\max} = n_2 \cdot pa \quad (8)$$

$$R = n_3 \cdot pa^2 \quad (9)$$

where n_1 , n_2 and n_3 are functions of the elastic restraint parameter K and the aspect ratio b/a of the lid. The values of n_1 , n_2 and n_3 associated with any given configuration can be obtained from Figures 5, 6 and 7, respectively.*

*In Figure 5 the data for a clamped plate ($K=\infty$, $\arctan K = \pi/2$) are taken from Table 35 of reference 2. All other data in this figure are based on the analysis in appendix A.

In Figure 6 the data for a simply supported plate ($\arctan K = 0$) are from Table 8 of reference 2. The data for a clamped plate ($\arctan K = \pi/2$) are based on the analysis in appendix B. The curves for elastically restrained plates ($\arctan K = .4, .8$ and 1.2) were inserted by interpolation assuming a linear variation of n_2 with respect to $\arctan K$, which is approximately the variation obtained for n_1 and n_3 . In view of the small change in n_2 in going from simple support to clamping (around 6% at the most) and the small role that n_2 will play in the subsequent development, this linear interpolation employed in Figure 6 is considered quite acceptable.

In Figure 7 the data for a simply supported plate ($\arctan K = 0$) are from Table 8 of reference 2. The remaining data are based on the analysis in appendix A.

The maximum deflection δ_{\max} of the lid under the lateral pressure p will occur at the center of the lid. The analysis of appendix A, which is based on small-deflection plate theory, gives

$$\delta_{\max} = n_4 \cdot \frac{pa^4}{D_c} = 12(1-\nu_c^2) \frac{p}{E_c} \left(\frac{a}{t}\right)^3 \cdot a \cdot n_4$$

where n_4 is a function of K and b/a to be obtained from Figure 8.* With ν_c approximated as 0.3, this becomes

$$\delta_{\max} = 10.92 n_4 \frac{p}{E_c} \left(\frac{a}{t}\right)^3 \cdot a$$

It is well known, however, that small-deflection theory tends to overestimate the deflection. Figure 9, therefore, presents a correction factor n_5 , based on large-deflection theory, to be applied to the right-hand sides of the above equations.** With this correction incorporated, the formula for maximum deflection now reads

$$\delta_{\max} = n_4 \cdot \frac{pa^4}{D_c} \cdot n_5 \quad (10)$$

or, with ν_c taken as 0.3,

$$\delta_{\max} = 10.92 n_4 \cdot \frac{p}{E_c} \left(\frac{a}{t}\right)^3 \cdot a \cdot n_5 \quad (10a)$$

For most packages K is likely to be very large, on the order of 100 or more, corresponding to nearly clamped conditions for the edges of the lid. In this range large changes in K , by a factor of 1/2 to 2, produce

*The data in Figure 8 for the cases $\arctan K = 0$ and $\pi/2$ are taken from Tables 8 and 35, respectively, of reference 2. The remaining data are based on the analysis in appendix A.

**Figure 9 applies rigorously only to the case $K = 0$, $\nu_c = 0.3$, but is probably sufficiently accurate for practical purposes for other values of K and ν_c as well. The solid curves of this figure are based on the table on page 181 of reference 3. The dashed curves are estimated interpolations or extrapolations due to the writer.

only small changes in $\arctan K$ (see Fig. 3) and, therefore, only small changes in n_1 , n_2 , n_3 and n_4 . This supports the assertion made earlier that the uncertainty regarding the exact value of α to be used in equation (4) will generally not have serious consequences.

FORMULAS FOR TENSILE STRESS IN THE SEAL

There are two conceivable locations for the maximum tensile stress in the seal: (a) in the middle of the long side, where the bending moment transmitted from the lid to the wall is a maximum; and (b) at the corners, where a reaction force R is developed to prevent the corners of the lid from lifting up. We shall consider these two locations separately.

Figure 10(a) shows the assumedly linear stress distribution across the width of the seal at the middle of the long side due to the bending moment M_{\max} alone, and Figure 10(b) shows the uniform compressive stress at the same location due to V_{\max} . Superposition of the two diagrams gives

$$S_{\text{edge}} = \frac{6 M_{\max}}{w^2} - \frac{V_{\max}}{w} \quad (11)$$

for the maximum tensile stress in the seal at the middle of the long side. It occurs at the outside edge of the seal. Substituting for M_{\max} and V_{\max} the expressions given in equations (7) and (8), one obtains

$$S_{\text{edge}} = p \left(\frac{a}{w} \right)^2 n_{\text{edge}} \quad (12)$$

where

$$n_{\text{edge}} = 6n_1 - n_2 \frac{w}{a} \quad (13)*$$

*Because of the factor w/a in equation (13), it is now evident that n_2 plays only a small role in determining the magnitude of the stress. Therefore, the simplifying assumption used in inserting the dashed curves in Figure 6 is quite acceptable.

Turning now to the corner, in order to estimate the stress due to the reaction R, one must make a reasonable assumption as to the area A over which this theoretically concentrated force is actually distributed. In the present work (see Fig. 11) A is assumed to be made up of the corner area w^2 , diminished by the area $(1 - \frac{\pi}{4})rw$ due to a possible small radius at the corner of the lid, and augmented by the area .47 tw along each side.* Thus,

$$A = w^2[1 + .94(t/w) - .21(r/w)^2] \quad (14)$$

In the event that the wall itself is rounded at the corners, as in Figure 12, the following formula should be used instead:

$$A = w^2[.79 + .94(t/w) + 1.57(r'/w)] \quad (15)$$

Both of these formulas can be represented by the single equation

$$A = w^2 n_6 \quad (16)$$

where

$$n_6 \equiv \begin{cases} 1 + .94(t/w) - .21(r/w)^2 & (17a) \\ \text{or} \\ .79 + .94(t/w) + 1.57(r'/w) & (17b) \end{cases}$$

the choice of (17a) or (17b) depending on whether the corner configuration is as shown in Figure 11 or Figure 12.

The tension stress in the seal at the corners can now be written as

$$S_{\text{corner}} = R/A \quad (18)$$

or, substituting for R and A their expressions from equations (9) and (16), respectively,

$$S_{\text{corner}} = p \left(\frac{a}{w}\right)^2 n_{\text{corner}} \quad (19)$$

*The dimension .47t in Figure 11 is based on some rather limited theoretical data from p. 173 of reference 2. There an analysis by A. Kromm is cited, for the case of a simply supported square plate with $a/t = 20$ and with deflections due to transverse shear taken into account, which leads to a high-intensity distributed reaction in place of the concentrated reaction R. The maximum intensity of this distributed reaction in that particular example can be correctly obtained by assuming the concentrated R of classical plate theory to be uniformly distributed of a total length of edge equal to .94 times the plate thickness.

where

$$n_{\text{corner}} \equiv n_3/n_6 \quad (20)$$

Equations (12) and (19) furnish two candidate values for the maximum tensile stress S_{max} in the seal. Thus

$$S_{\text{max}} = p \left(\frac{a}{w} \right)^2 n_{\text{max}} \quad (21)$$

where

$$n_{\text{max}} \equiv \text{the larger of } n_{\text{edge}} \text{ and } n_{\text{corner}} \quad (22)$$

For most designs n_{edge} will govern in equation (22).

APPLICATION TO DESIGN AND SCREENING

The formulas developed above can be of use both to the designer, whose objective is to design a package that will remain hermetic under a specified screening pressure, and the user, whose objective is to select an appropriate screening pressure that will destroy the hermeticity of packages with poor quality seals.

Application to design: Considering first the designer, let it be supposed that he knows the sealing material to be used and has a value of the allowable tensile stress S_{all} for that material. Then his criterion for a satisfactory design, from the point of view of retaining hermeticity under external pressure, should be that S_{max} , as given by equation (21), is less than S_{all} . That is,

$$p \left(\frac{a}{w} \right)^2 n_{\text{max}} \leq S_{\text{all}} \quad (23)$$

where p is the largest anticipated screening pressure. In selecting S_{all} the designer should, of course, be conservative. If S_{all} is taken as the

median tensile strength of the sealing material, as obtained from a number of tests of that material alone, then packages designed on the basis of the equality sign in equation (23) will have a failure rate of approximately 50% even if properly sealed (and a higher failure rate if there is a mixture of properly and improperly sealed packages). On the other hand, if the designer selects for S_{a11} the 1-percentile value of the tensile strengths obtained in a large number of tests of the sealing material alone, then he should expect only a 1% failure rate for properly sealed packages designed on the basis of equation (23) with the equality sign.

It could happen that the designer has very little data on the distribution of tensile strength values for the sealing material, or even on the mean strength, but he does know that a certain previously designed package, designated as I, when properly sealed with the same material had an acceptable failure rate F under a screening pressure of p_I . Then in order for the new package, designated as II, to have a failure rate no greater than F when properly sealed and subjected to its screening pressure p_{II} , he should so design package II that its S_{max} is no greater than that of package I. Thus, referring to equation (21), his criterion for a satisfactory design of package II should be

$$p_{II} \left[\left(\frac{a}{w} \right)^2 n_{max} \right]_{II} \leq p_I \left[\left(\frac{a}{w} \right)^2 n_{max} \right]_I \quad (24)$$

$$\text{or} \quad \left[\left(\frac{a}{w} \right)^2 n_{max} \right]_{II} \leq \frac{p_I}{p_{II}} \left[\left(\frac{a}{w} \right)^2 n_{max} \right]_I \quad (24a)$$

If the same screening pressure is to be used for package II as for package I, this design criterion becomes

$$\left[\left(\frac{a}{w} \right)^2 n_{\max} \right]_{II} \leq \left[\left(\frac{a}{w} \right)^2 n_{\max} \right]_I \quad (24L)$$

Application to screening: Turning now to the user of an already designed package, let us first suppose that he has a minimum acceptable value, S_{accept} , for the tensile strength of the seal and wants to be sure of rejecting all packages with seal strengths less than that. Then he should select a screening pressure p such that the S_{max} defined by equation (21) is equal to or greater than S_{accept} . Thus, the required screening pressure is defined by

$$p \geq \frac{S_{\text{accept}}}{\left(\frac{a}{w} \right)^2 n_{\max}} \quad (25)$$

It is more than likely, however, that the user of the package will not have enough information about the sealing material to be able to specify a value for S_{accept} , but he might know that in the past a certain pressure p_I was considered suitable for the screening of a certain package, designated as I, employing the same sealing material as the present package, which we shall designate as II. Then his criterion for selecting a suitable screening pressure p_{II} for the present package should be that the S_{max} of package II, under the pressure p_{II} , be at least as big as the S_{max} of package I under the pressure p_I . Referring again to equation (21), we see that the criterion for selecting p_{II} is then

$$p_{II} \left[\left(\frac{a}{w} \right)^2 n_{\max} \right]_{II} \geq p_I \left[\left(\frac{a}{w} \right)^2 n_{\max} \right]_I \quad (26)$$

or

$$P_{II} \geq P_I \frac{\left[\left(\frac{a}{w} \right)^2 n_{\max} \right]_I}{\left[\left(\frac{a}{w} \right)^2 n_{\max} \right]_{II}} \quad (26a)$$

Possible modification in above procedures: In appendix C some doubts are raised as to the validity of the corner stress. Theoretical arguments are presented which indicate that equation (19) might over-estimate this stress and that, in fact, this stress might not exist at all. Thus, there is an uncertainty regarding the existence of the corner stress, and the question naturally arises what modifications, if any, are needed in the designing and screening recommendations just presented because of this uncertainty.

In the writer's opinion, the answer to this question should be as follows: One should accept or discount the existence of the corner stress on the basis of which attitude will lead to the more conservative result. For the designer this means that if he is designing on the basis of equation (23) he should use that equation as it stands; but if designing on the basis of equation (24), (24a) or (24b), he should make sure that the inequality remains satisfied with n_{\max} replaced by n_{edge} on both sides. On the other hand, the user of the package, who is trying to arrive at a proper screening pressure p , would make two calculations, one on the assumption that the corner stress exists, the other on the assumption that it does not exist, and use the higher of the two pressures thus obtained. The first calculation is the one already described above; that is, it is a calculation based on equation (25) or (26a). For the second calculation equation (25) or (26a) is again used, but with n_{\max} replaced by n_{edge} .

Fortunately, for most packages S_{edge} , as given by equation (12), will be much greater than S_{corner} , as given by equation (19). Thus, in most cases the question as to whether equation (19) over-estimates S_{corner} or whether S_{corner} actually exists will be academic, and the modified designing and screening procedures will be in no way different from the original procedures.

Lid deflection: It goes without saying that the designer and the user both must concern themselves with the center deflection of the lid, in order to insure that during any screening the deflection will not be so large as to produce contact between the lid and the contents of the package. The pertinent formula for estimating center deflection is equation (10a). The designer should so design the package that under the anticipated screening pressure this deflection is less than the anticipated internal clearance between lid and contents. By the same token, the user, after tentatively selecting a screening pressure, should compute the center deflection produced by that pressure and make sure that it does not exceed the internal clearance. If it does, then he may have to use a less severe screening pressure (i.e., accept a higher risk of non-hermeticity) in order not to jeopardize the integrity of the contents of the package in the screening.

FLAT-PACKS IN A CENTRIFUGE

As part of the total screening process, packages are frequently spun in a centrifuge in such a way that the centrifugal force tends to push the lid into the cavity. As far as the lid alone is concerned, this

centrifugal force is equivalent to a lateral pressure of magnitude Gtd , where G is centripetal acceleration in units of g (acceleration of gravity, 32.2 ft./sec.^2), t is the lid thickness, and d is the specific weight (weight per unit volume) of the lid material. If t is in inches and d in lbs. per cubic inch, the formula

$$p = Gtd \quad (27)$$

will give the effective pressure, in psi, due to a centrifuge acceleration of G g's.

Thus, the formulas developed in the preceding sections can be made to apply to a package in a centrifuge simply by replacing the symbol p everywhere by Gtd . In this way, for example, the following formula is obtained from equation (10a) for the central deflection of the lid of a package in a centrifuge:

$$\delta_{\max} = 10.92 n_4 \frac{Gtd}{E_c} \left(\frac{a}{t}\right)^3 \cdot a \cdot n_5 \quad (28)$$

From equations (12), (19) and (21) the following formulas are obtained for the tensile stresses in the seal:

$$S_{\text{edge}} = Gtd \left(\frac{a}{w}\right)^2 n_{\text{edge}} \quad (29)$$

$$S_{\text{corner}} = Gtd \left(\frac{a}{w}\right)^2 n_{\text{corner}} \quad (30)$$

$$S_{\max} = Gtd \left(\frac{a}{w}\right)^2 n_{\max} \quad (31)$$

It should be noted that the interaction among the base, walls, and lid of a package may be somewhat different for a package in a centrifuge than for the same package under a uniform hydrostatic pressure. Therefore, the value of α to be used in equations (4) to (3a) is not necessarily the same for the package in the centrifuge as it is for the same package

under hydrostatic pressure. As an aid in estimating the appropriate value of α let us consider one extreme condition, illustrated in Figure 14(a). In this figure the lid and base are assumed to be identical and the package is assumed to be supported in the centrifuge only at its edges. Under these circumstances the lid and base will deform identically under their centrifugal loadings and the walls will develop lines of contraflexure at mid-height. It can be shown that the appropriate value for α is then 6. A more likely support condition is illustrated in Figure 14(b). There the base is firmly bonded to a flat surface, producing an essentially clamped condition for the bottom edges of the walls. In this case α should be taken as 4. Again it should be noted that for most packages this uncertainty in the value of α is of no real consequence.

Equations (28) to (30) can be used to determine if any undesirable lid deflection or seal stresses will result from a given centrifuge acceleration. Equation (27) can be used in the following way: If a certain hydrostatic pressure p is known to be destructive of lid or seal for a given package, then equation (27), rewritten as

$$G = \frac{p}{td} \quad (32)$$

will give the acceleration (in g's) that will produce approximately the same destructive effects. Conversely, if a certain hydrostatic pressure is known to be non-destructive of lid or seal then equation (32) can be used to estimate a value of G that will also be non-destructive.

To gain further insight into the equivalence of hydrostatic pressure and constant acceleration, let us consider a lid of .030 in. thickness and .302 lbs. per cu. in. density and ask how many g's of centrifuge

acceleration are equivalent to a lateral pressure of 30 psi on the lid.

From equation (32) the answer is

$$G = \frac{30}{(.030)(.302)} = 3310 \text{ (g's)}$$

NUMERICAL EXAMPLES

Example 1. A package has the following properties: $a = b = 1.000$ in., $t = .015$ in., $h = .105$ in., $w = .040$ in., $r = .010$ in., $E_c = E_w = 20,000,000$ psi, $\nu_c = \nu_w = 0.3$, $d = .302$ lb./in.³. What are the maximum tensile stress in the seal and the central deflection of the lid due to an external pressure of 30 psi?

With α assumed to be 3, equation (6a) gives

$$K^1 = 3 \left(\frac{.040}{.015} \right)^3 \frac{1.000}{.105} = 541 \quad (33)$$

Figure 3 then gives $\arctan K = 1.57$ (that is, the lid is essentially clamped along its edges). Entering Figures 5, 6, 7 and 8 with $b/a = 1$ and $\arctan K = 1.57$, one obtains

$$n_1 = .051, n_2 = .443, n_3 = 0, n_4 = .00125 \quad (34)$$

For $p = 30$ psi,

$$\frac{pa^4}{E_c t^4} = \frac{30}{20,000,000} \left(\frac{1}{.015} \right)^4 = 29.6 \quad (35)$$

Therefore (Fig. 9)

$$n_5 = .825 \quad (36)$$

Equation (10a) now gives the following lid deflection:

$$\begin{aligned} \delta_{\max} &= 10.92(.00125) \frac{30}{20,000,000} \left(\frac{1}{.015} \right)^3 (1.000 \text{ in.})(.825) \\ &= \underline{\underline{.0050 \text{ in.}}} \end{aligned} \quad (37)$$

From equations (13), (17a), (20) and (22) there follows

$$\begin{aligned}n_{\text{edge}} &= 6(.051) - (.443) \frac{.040}{1.000} = .288 \\n_6 &= 1 + .94 \left(\frac{.015}{.040} \right) - .21 \left(\frac{.010}{.040} \right)^2 = 1.34 \\n_{\text{corner}} &= 0 \\n_{\text{max}} &= .288\end{aligned}\tag{38}$$

Thus, the maximum tensile stress in the seal occurs at the middle of the long edge. Its value, from equation (21), is

$$S_{\text{max}} = 30 \left(\frac{1.000}{.040} \right)^2 (.288) \cdot \underline{\underline{5,400 \text{ psi}}}\tag{39}$$

Example 2. Suppose that 30 psi is considered a satisfactory screening pressure for the package of Example 1 (to be referred to as package I), what screening pressure would be appropriate for a second package (package II) identical in all respects to package I except for the length b, which is 2.000 in.? What will the lid deflection be under this screening pressure?

For package II we have $b/a = 2$ and $\arctan K$ still equal to 1.57.

Figures 5, 6, 7 and 8 then give the following information for this package:

$$n_1 = .083, n_2 = .51, n_3 = 0, n_4 = .00255\tag{40}$$

Also, from equations (13), (17a), (20) and (22),

$$\begin{aligned}n_{\text{edge}} &= 6(.083) - (.51) \frac{.040}{1.000} = .477 \\n_6 &= 1.34 \\n_{\text{corner}} &= 0 \\n_{\text{max}} &= .477\end{aligned}\tag{41}$$

Equation (26a) now gives

$$p_{II} = 30 \cdot \frac{\left(\frac{1.000}{.040}\right)^2 (.288)}{\left(\frac{1.000}{.040}\right)^2 (.477)} = \underline{\underline{18 \text{ psi}}} \quad (42)$$

as the appropriate screening pressure for package II. For this pressure

$$\frac{pa^4}{E_c t^4} = \frac{18}{20,000,000} \left(\frac{1.000}{.015}\right)^4 = 17.9 \quad (43)$$

The curve for $b/a = 2$ in Figure 9 then gives

$$n_5 = .87 \quad (44)$$

From equation (10a) the center deflection of the lid of package II under a screening pressure of 18 psi is now found to be

$$\begin{aligned} \delta_{\max} &= 10.92(.00255) \frac{18}{20,000,000} \left(\frac{1.000}{.015}\right)^3 (1.000 \text{ in.})(.87) \\ &= \underline{\underline{.0065 \text{ in.}}} \end{aligned}$$

Example 3. For the package of Example 1 a maximum tensile stress of 5,400 psi in the seal material was computed for a screening pressure of 30 psi. Suppose that the maximum permissible stress in the seal is 4,500 psi, what new lid thickness (if any) would reduce S_{\max} to this value, all other dimensions remaining unchanged?

Assume, tentatively, that S_{\max} will still occur along the edge, rather than at the corner. Then the criterion for a satisfactory design, from equation (23) with n_{\max} set equal to n_{edge} , is

$$n_{\text{edge}} \leq \frac{S_{\text{all}}}{p \left(\frac{a}{w}\right)^2} = \frac{4500}{30 \left(\frac{1.000}{.040}\right)^2} = .24$$

In view of equation (13) this criterion may be written as

$$6n_1 - n_2 \frac{w}{a} \leq .24 \quad (45)$$

or, substituting for w/a its value of .040 and solving for n_1 ,

$$n_1 \leq .040 + .0067 n_2 \quad (46)$$

The value of n_2 is fairly insensitive to K (see Fig. 6) and, therefore, very little error is involved if we continue to use for n_2 the value found for it in Example 1, namely .443. Thus, equation (46) becomes

$$n_1 \leq .043 \quad (47)$$

Referring to the curve for $b/a = 1$ in Figure 5, we see that this requires

$$\arctan K \leq 1.45 \quad (48)$$

or, from Figure 3,

$$K^1 \leq 20 \quad (49)$$

Substituting for K^1 its expression from equation (6a), and using the numerical data specified in Example 1, we convert this to

$$3\left(\frac{w}{t}\right)^3 \frac{1.000}{.105} \leq 20 \quad (50)$$

whence

$$\frac{w}{t} \leq .888$$

or

$$t \geq \frac{w}{.888} = \frac{.040}{.888} = .045 \text{ in.} \quad (51)$$

Thus, a lid thickness comparable to the wall thickness would be needed to reduce the maximum tensile stress in the seal at the middle of the side to 4500 psi.

The corner stress in the seal must now be checked to see that it does not exceed the maximum permissible stress of 4500 psi. From

equations (19), (20) and (17a), we have

$$S_{\text{corner}} = p \left(\frac{a}{w} \right)^2 \frac{n_3}{1 + .94 \frac{t}{w} - .21 \left(\frac{x}{w} \right)^2} \quad (52)$$

For $\arctan K = 1.45$ and $b/a = 1.0$, Figure 7 gives

$$n_3 = .0056 \quad (53)$$

Substituting this into equation (52) together with the numerical values of the other parameters, we have

$$S_{\text{corner}} = 30 \left(\frac{1.000}{.040} \right)^2 \frac{.0056}{1 + .94 \left(\frac{.097}{.040} \right) - .21 \left(\frac{.010}{.040} \right)^2} = 32 \text{ psi} \quad (54)$$

which is indeed less than the 4500 psi allowable.

CONCLUDING REMARKS

Formulas based on classical plate theory have been presented for the reactions and center deflection of the lid of a rectangular flat-pack under external pressure, and suggestions have been made as to how these formulas can be of use in the design and screening of flat-packs.

There are several simplifying assumptions underlying the present work. Most of them have already been discussed and justified. One which has not yet been discussed, and which warrants close scrutiny, is the second hypothesis stated in the Introduction; namely, that the screening effectiveness of external pressure in weeding out non-hermetic or potentially non-hermetic seals is due to the tensile stresses which this pressure produces in the seal material. This hypothesis is admittedly debatable. One could argue that the screening action is due to the

seepage of fluid into the package through pre-existing voids or narrow passages in seals of poor quality. Undoubtedly, some of the screening action is due to such seepage, but the writer feels that the tensile stresses produced by the pressure are the predominant screening mechanism. There is some evidence to support this feeling: Firstly, those who are knowledgeable in the screening of flat-packs report that the screening power (failure rate) of external pressure goes up drastically as the package size (dimensions a and b) increases. This is consistent with equation (21), which shows that the maximum tensile stress in the seal is approximately proportional to the square of the dimension a. Secondly, p. 5 of reference 4 describes the "pressure withstanding capability" of properly sealed Bendix packages as follows:

<u>Holder Size</u>	<u>Pressure Differential</u>
3/8 square	5 atmospheres
3/8 to 5/8 square	3 atmospheres
5/8 to 3/4 square	2 atmospheres
3/4 square	1.25 atmospheres

We note that as the size is doubled (going from 3/8 square to 3/4 square), the allowable pressure differential is reduced by a factor of 4 (from 5 atmospheres to 1.25 atmospheres). Equation (26a) predicts approximately the same relationship between package size and screening pressure.

A second assumption which warrants further attention is the one illustrated in Figure 10(a); namely, that the bending moment at the edge of the lid produces a linear variation of stress across the width of the seal, as in elementary beam theory. This kind of assumption is frequently made; it follows from the assumption of plane horizontal sections through the seal remaining plane and the assumption of Hooke's law. As the

stresses in the seal material becomes high we can expect that plastic behavior and possibly creep in the seal material will destroy the linearity in the stress distribution and reduce the maximum stress. Furthermore, if the lid is thin compared to the thickness of the wall ($t \ll w$), we should not expect the lid to be able to enforce the plane sections assumption in the seal. For $t \ll w$ the action of that portion of the lid in contact with the seal would probably be like that of a beam attached to an elastic foundation, and the pressure distribution between such a beam and its foundation is known to be non-linear. Thus, the linear-stress-distribution assumption of Figure 10(a) has obvious shortcomings. Nevertheless, it has been employed in the hope that it may be sufficiently good for practical purposes and because any more sophisticated assumption would involve an inordinate amount of additional analysis.

A third assumption implicit in the present work is that the pressure on the side walls makes a negligible contribution to the stresses in the seal. For shallow packages the validity of this assumption is intuitively evident. A semi-quantitative justification of it can be made by analyzing the configuration of Figure 1(b) as a rigid-jointed plane frame under pressure on the vertical members alone and pressure on the horizontal members alone. Such an analysis shows that the ratio of the corner bending moment due to side-wall pressure alone to the corner bending moment due to pressure on the top and bottom covers alone is of the order of $D_c h^3 / D_w a^3$ or $(E_c / E_w) (t^3 / w^3) (h^3 / a^3)$. For any flat-pack of practical design this ratio will be much smaller than unity, indicating that the side-wall

pressure makes a negligible contribution to the bending moment transmitted across the seal and, therefore, to the stress in the seal.

The final test of the validity of any theoretical work and the hypotheses on which it is based must, of course, be based on experiments. In the present case one can envision a modest experimental program that could provide evidence as to the validity of the assumptions that have been made. This program would require flat-packs of different sizes and shapes, all carefully sealed with the same material. The value of n_{\max} (eq. (22)) would be computed for each package. Each package would then be subjected to external pressure which is increased in small steps, and the pressure p_{cr} which first causes a loss of hermeticity would be noted. The product $p_{cr} (a/w)^2 n_{\max}$ would then be computed for each package. According to equation (21), this product represents the maximum tensile stress in the seal at the time of loss of hermeticity. If the seals are of reasonably uniform quality, so that they all have essentially the same tensile strength S_{ult} , and if the hypothesis of this report (to the effect that failure occurs when $S_{\max} = S_{ult}$) is correct, then this product should turn out to be approximately the same for all packages.

If the test program just described tends to confirm the present hypotheses, then a second program would be desirable, identical to the first, except that the seal material would be changed to one of much higher or much lower strength. The purpose of this program would be to see if there is a corresponding change in the experimental values of $p_{cr} (a/w)^2 n_{\max}$, as there should be if the failure hypothesis $S_{\max} = S_{ult}$ is correct.

APPENDIX A

SMALL-DEFLECTION ANALYSIS OF A UNIFORMLY LOADED ELASTIC RECTANGULAR PLATE WITH EDGES ELASTICALLY RESTRAINED AGAINST ROTATION

Here the energy method will be employed, in conjunction with double Fourier series and Lagrangian multipliers, to obtain the deflections and other quantities of interest in a uniformly loaded elastic rectangular plate with edges elastically restrained against rotation.

Coordinate system and notation.— We shall employ the coordinate system and notation shown in Figure 4 and let $w(x,y)$ denote the deflection of the plate, positive if in the same direction as the pressure, p . The following additional symbols will be used:

k = elastic restraint stiffness (moment per unit length per radian of rotation).

E = Young's modulus of plate material.

ν = Poisson's ratio.

$D \equiv Et^3/[12(1-\nu^2)]$.

$K \equiv 4ak/(\pi^2 D)$.

$\beta \equiv a/b$.

Series for w and its second derivatives.— The double Fourier series

$$w(x,y) = \sum_{m=1,3,\dots}^M \sum_{n=1,3,\dots}^N a_{mn} \sin(m\pi x/a) \sin(n\pi y/b) \quad (A1)$$

is an appropriate representation of the deflections of a rectangular plate with zero deflection at the edges. Only odd values of the

summation indices m and n are taken in equation (A1) because under uniform pressure the deflections will be symmetric with respect to the planes $x=a/2$ and $y=b/2$. Upper limits M and N are shown for the summations with the understanding that in the computations M and N will be assigned sufficiently high values to establish practical convergence for all quantities of interest.

The boundary condition of zero deflection at the edges permits one to obtain $\partial^2 w / \partial x^2$, $\partial^2 w / \partial y^2$, and $\partial^2 w / \partial x \partial y$ by termwise differentiations of equation (A1). Consequently,

$$\begin{aligned} \frac{\partial^2 w}{\partial x^2} &= - \sum_{m=1,3,\dots}^M \sum_{n=1,3,\dots}^N a_{mn} (m\pi/a)^2 \sin(m\pi x/a) \sin(n\pi y/b) \\ \frac{\partial^2 w}{\partial y^2} &= - \sum_{m=1,3,\dots}^M \sum_{n=1,3,\dots}^N a_{mn} (n\pi/b)^2 \sin(m\pi x/a) \sin(n\pi y/b) \quad (A2) \\ \frac{\partial^2 w}{\partial x \partial y} &= \sum_{m=1,3,\dots}^M \sum_{n=1,3,\dots}^N a_{mn} (m\pi/a) (n\pi/b) \cos(m\pi x/a) \cos(n\pi y/b) \end{aligned}$$

Series for edge rotations.— The rotations $\theta_1(x)$ of the edge $y=0$ and $\theta_2(y)$ of the edge $x=0$ will be represented in the form of single series:

$$\theta_1(x) = \sum_{m=1,3,\dots}^M b_m \sin(m\pi x/a) \quad \theta_2(y) = \sum_{n=1,3,\dots}^N c_n \sin(n\pi y/b) \quad (A3)$$

Constraining relations.— The deflections $w(x,y)$ and the rotations $\theta_1(x)$ and $\theta_2(y)$ must satisfy the following compatibility conditions:

$$(\partial w / \partial y)_{y=0} = \theta_1(x) \quad (\partial w / \partial x)_{x=0} = \theta_2(y)$$

These give rise to the following constraining relations among the

Fourier coefficients a_{mn} , b_m , c_n :

$$\sum_{n=1,3,\dots}^N a_{mn} \frac{n\pi}{b} - b_m = 0 \quad (m=1,3,\dots,M) \quad (A4)$$

$$\sum_{m=1,3,\dots}^M a_{mn} \frac{m\pi}{a} - c_n = 0 \quad (n=1,3,\dots,N)$$

Strain energy of plate.— The strain energy integral for a rectangular elastic plate undergoing small deflections is given on page 342 of reference 2. There it is also shown that substitution of the series (A1) into the strain energy integral leads to the following formula for the strain energy V_1 of the plate:

$$V_1 = \frac{\pi^4 abD}{8} \sum_{m=1,3,\dots}^M \sum_{n=1,3,\dots}^N a_{mn}^2 \left(\frac{m^2}{a^2} + \frac{n^2}{b^2} \right)^2 \quad (A5)$$

Strain energy of elastic restraint.— The strain energy V_2 of the rotational elastic restraint along the edges of the plate can be written

as

$$V_2 = 2 \left\{ \frac{1}{2} k \int_0^a [\theta_1(x)]^2 dx + \frac{1}{2} k \int_0^b [\theta_2(y)]^2 dy \right\}$$

Substitution of the series (A3) for $\theta_1(x)$ and $\theta_2(y)$ leads to

$$V_2 = \frac{1}{2} ka \sum_{m=1,3,\dots}^M b_m^2 + \frac{1}{2} kb \sum_{n=1,3,\dots}^N c_n^2 \quad (A6)$$

Potential energy of the applied load.— Taking the xy-plane taken as datum, one may express the potential energy V_3 of the applied load as

$$V_3 = -p \iint w dx dy$$

or, substituting for w its series expression,

$$V_3 = - \frac{4pab}{\pi} \sum_{m=1,3,\dots}^M \sum_{n=1,3,\dots}^N \frac{a_{mn}}{mn} \quad (A7)$$

Minimization of the total potential energy.— The total potential energy (TPE) of the system consisting of the plate, its loading, and the elastic constraints is defined as

$$TPE = V_1 + V_2 + V_3 \quad (A8)$$

According to the principle of minimum total potential energy for elastic structures, the true configuration of the system, among all possible configurations satisfying continuity and any rigid constraints, is that which minimizes the TPE. Thus, the correct values of the a_{mn} , b_m and c_n are those which minimize expression (A8) while at the same time satisfying the constraining relations (A4). This "constrained minimization" problem can be solved by setting up the new function

$$\begin{aligned} TPE^* = V_1 + V_2 + V_3 - \sum_{m=1,3,\dots}^M \alpha_m \left(\sum_{n=1,3,\dots}^N a_{mn} \frac{n\pi}{b} - b_m \right) \\ - \sum_{n=1,3,\dots}^N \beta_n \left(\sum_{m=1,3,\dots}^M a_{mn} \frac{m\pi}{a} - c_n \right) \end{aligned} \quad (A9)$$

where the α_m and β_n are Lagrangian multipliers, and making it stationary with respect to the a_{mn} 's, the b_m 's, the c_n 's, the α_m 's, and the β_n 's via the following conditions:

$$\partial(TPE^*)/\partial a_{ij} = 0 \quad (i=1,3,\dots,M; j=1,3,\dots,N) \quad (A10)$$

$$\partial(TPE^*)/\partial b_i = 0 \quad (i=1,3,\dots,M) \quad (A11)$$

$$\partial(TPE^*)/\partial c_j = 0 \quad (j=1,3,\dots,N) \quad (A12)$$

$$\partial(TPE^*)/\partial\alpha_1 = 0 \quad (i=1,3,\dots,M) \quad (A13)$$

$$\partial(TPE^*)/\partial\beta_j = 0 \quad (j=1,3,\dots,N) \quad (A14)$$

(Equations (A13) and (A14) merely replicate the constraining relations (A4).) With the differentiations carried out and some minor algebraic manipulations executed, (A10) to (A14) become:

$$A_{ij} = \frac{1 + j^2 A_1 + i^2 B_j}{ij(1^2 + j^2 \beta_j^2)^2} \quad (i=1,3,\dots,M; j=1,3,\dots,N) \quad (A15)$$

$$b_i^* = -A_1/K \quad (i=1,3,\dots,M) \quad (A16)$$

$$c_j^* = -B_j/K \quad (j=1,3,\dots,N) \quad (A17)$$

$$b_i^* - i\beta^3 \sum_{j=1,3,\dots}^N jA_{ij} = 0 \quad (i=1,3,\dots,M) \quad (A18)$$

$$c_j^* - j \sum_{i=1,3,\dots}^M iA_{ij} = 0 \quad (j=1,3,\dots,N) \quad (A19)$$

where A_{ij} , A_1 , B_j , b_i^* , c_j^* , and K are dimensionless measures of a_{ij} , α_1 , β_j , b_i , c_j , and k , defined as follows:

$$A_{ij} = \pi^6 D a_{ij} / 16 a^4 p \quad (A20)$$

$$A_1 = i\pi^3 \alpha_1 / 4 a b^2 p \quad (A21)$$

$$B_j = j\pi^3 \beta_j / 4 a^2 b p \quad (A22)$$

$$b_i^* = i\pi^5 D b_i / 16 a b^2 p \quad (A23)$$

$$c_j^* = j\pi^5 D c_j / 16 a^3 p \quad (A24)$$

$$K = 4ka/\pi^2 D \quad (A25)$$

Equations (A15) through (A19) are a system of simultaneous linear algebraic equations defining the A_{ij} , A_i , B_j , b_i^* , and c_j^* .

Simplification of simultaneous equations.— Equations (A15), (A16) and (A17) can be used to eliminate the A_{ij} , b_i^* and c_j^* in (A18) and (A19). The latter then becomes:

$$A_i + \beta^3 K \sum_{j=1,3,\dots}^N \frac{1 + j^2 A_i + i^2 B_j}{(i^2 + j^2 \beta^2)^2} = 0 \quad (i=1,3,\dots,M) \quad (A26)$$

$$B_j + K \sum_{i=1,3,\dots}^M \frac{1 + j^2 A_i + i^2 B_j}{(i^2 + j^2 \beta^2)^2} = 0 \quad (j=1,3,\dots,N) \quad (A27)$$

A further reduction in the number of simultaneous equations is effected as follows: Solve (A27) for each B_j in terms of all the A_i to get

$$B_j = \frac{f_2(j)}{f_1(j)} - \frac{j^2}{f_1(j)} \sum_{q=1,3,\dots}^M \frac{A_q}{(q^2 + j^2 \beta^2)^2} \quad (j=1,3,\dots,N) \quad (A28)$$

where

$$f_1(j) \equiv K^{-1} + \sum_{i=1,3,\dots}^M i^2 (i^2 + j^2 \beta^2)^{-2} \quad (A29)$$

$$f_2(j) \equiv - \sum_{i=1,3,\dots}^M (i^2 + j^2 \beta^2)^{-2}$$

Now use (A28) to eliminate the B_j 's in (A26) and thereby arrive at the following system of simultaneous equations in the A_i 's alone:

$$\sum_{q=1,3,\dots}^M A_q f_6(i,q) = f_7(i) \quad (i=1,3,\dots,M) \quad (A30)$$

where

$$f_6(i, q) = \delta_{iq} [(\beta^3 K)^{-1} + \sum_{j=1,3,\dots}^N j^2 (i^2 + j^2 \beta^2)^{-2}] - i^2 \sum_{j=1,3,\dots}^N j^2 (q^2 + j^2 \beta^2)^{-2} (i^2 + j^2 \beta^2)^{-2} [f_1(j)]^{-1} \quad (A31)$$

$$f_7(i) = - \sum_{j=1,3,\dots}^N (i^2 + j^2 \beta^2)^{-2} \{1 + i^2 f_2(j) [f_1(j)]^{-1}\} \quad (A32)$$

with δ_{iq} being Kronecker's delta.

On the basis of these transformations, we now have the following calculation procedure: Solve equations (A30) (whose number depends only on M, not on N) simultaneously for the A_q 's and substitute their values into (A28) to obtain the B_j 's. (In the special case $k=0$ the A_q 's and the B_j 's are identically zero (see eqs. (A26) and (A27)). With the A_q 's and B_j 's known, equations (A15) will yield the values of the A_{ij} 's.

Once the above quantities have been determined, all other items of interest can be computed, as will be seen in the following sections.

Center deflection.— Equation (A1), evaluated at $x=a/2$, $y=b/2$, gives

$$w\left(\frac{a}{2}, \frac{b}{2}\right) = \frac{16a^4 p}{\pi^6 E} \sum_{m=1,3,\dots}^M \sum_{n=1,3,\dots}^N A_{mn} (-1)^{\frac{m+n-2}{2}} \quad (A33)$$

Corner reaction.— From page 85 of reference 2 we have the following equation for the corner reaction in terms of the corner rate of twist:

$$R = 2D(1-\nu) \left(\partial^2 w / \partial x \partial y \right)_{\substack{x=0 \\ y=0}}$$

Elimination of the twist through equation (A2) then gives

$$R = pa^2 \cdot 32(1-\nu)\beta\pi^{-4} \sum_{m=1,3,\dots}^M \sum_{n=1,3,\dots}^N A_{mn} mn \quad (A34)$$

Bending moments along the sides.— The bending moments normal to the edges $y=0$ and $x=0$ are related to the rotation functions $\theta_1(x)$ and $\theta_2(y)$ as follows:

$$(M_y)_{y=0} = -k\theta_1(x) \quad (A35)$$

$$(M_x)_{x=0} = -k\theta_2(y)$$

Substituting for $\theta_1(x)$ and $\theta_2(y)$ their series expansions (A3) and making use of the relations (A16) and (A17), one obtains

$$(M_y)_{y=0} = \frac{4pb^2}{\pi^3} \sum_{m=1,3,\dots}^M \frac{A_m \sin(m\pi x/a)}{m} \quad (A36)$$

$$(M_x)_{x=0} = \frac{4pa^2}{\pi^3} \sum_{n=1,3,\dots}^N \frac{B_n \sin(n\pi y/b)}{n}$$

Curvatures along the sides.— The curvatures normal to the edges can now be determined from the moment-curvature relations and equations (A36) as follows:

$$\left(\frac{\partial^2 w}{\partial y^2} \right)_{y=0} = -\frac{1}{D}(M_y)_{y=0} = -\frac{4pb^2}{\pi^3 D} \sum_{m=1,3,\dots}^M \frac{A_m \sin(m\pi x/a)}{m} \quad (A37)$$

$$\left(\frac{\partial^2 w}{\partial x^2} \right)_{x=0} = -\frac{1}{D}(M_x)_{x=0} = -\frac{4pa^2}{\pi^3 D} \sum_{n=1,3,\dots}^N \frac{B_n \sin(n\pi y/b)}{n}$$

Some third derivatives of w. - Termwise differentiation of the Fourier series (A1) is permissible in order to arrive at the following series expansions:

$$\begin{aligned}\frac{\partial^3 w}{\partial x \partial y^2} &= - \sum_{m=1,3,\dots}^M \sum_{n=1,3,\dots}^N a_{mn} \left(\frac{n\pi}{b}\right)^2 \left(\frac{m\pi}{a}\right) \cos \frac{m\pi x}{a} \sin \frac{n\pi y}{b} \\ \frac{\partial^3 w}{\partial x^2 \partial y} &= - \sum_{m=1,3,\dots}^M \sum_{n=1,3,\dots}^N a_{mn} \left(\frac{m\pi}{a}\right)^2 \left(\frac{n\pi}{b}\right) \sin \frac{m\pi x}{a} \cos \frac{n\pi y}{b}\end{aligned}\quad (A38)$$

Termwise differentiation is, however, not valid for obtaining $\partial^3 w / \partial x^3$ and $\partial^3 w / \partial y^3$. We therefore postulate the new series

$$\begin{aligned}\frac{\partial^3 w}{\partial x^3} &= \sum_{m=1,3,\dots}^M \sum_{n=1,3,\dots}^N b_{mn} \cos \frac{m\pi x}{a} \sin \frac{n\pi y}{b} \\ \frac{\partial^3 w}{\partial y^3} &= \sum_{m=1,3,\dots}^M \sum_{n=1,3,\dots}^N c_{mn} \sin \frac{m\pi x}{a} \cos \frac{n\pi y}{b}\end{aligned}\quad (A39)$$

from which it follows that

$$\begin{aligned}b_{mn} &= \frac{4}{ab} \int_0^b \int_0^a \frac{\partial^3 w}{\partial x^3} \cos \frac{m\pi x}{a} \sin \frac{n\pi y}{b} dx dy \\ c_{mn} &= \frac{4}{ab} \int_0^a \int_0^b \frac{\partial^3 w}{\partial y^3} \cos \frac{n\pi y}{b} \sin \frac{m\pi x}{a} dy dx\end{aligned}\quad (A40)$$

Partial integration with respect to x in the first of these equations gives

$$b_{mn} = -\frac{4}{a} \left[\frac{2}{b} \int_0^b \left(\frac{\partial^2 w}{\partial x^2} \right)_{x=0} \sin \frac{n\pi y}{b} dy \right] + \frac{m\pi}{a} \left[\frac{4}{ab} \iint \frac{\partial^2 w}{\partial x^2} \sin \frac{m\pi x}{a} \sin \frac{n\pi y}{b} dx dy \right] \quad (A41)$$

The first bracketed term will be recognized as the formula for the Fourier coefficient in the sine series for $(\partial^2 w / \partial x^2)_{x=0}$, and therefore, referring to equations (A37), it may be replaced by

$$-\frac{4pa^2}{\pi^3 D} \cdot \frac{B_n}{n}$$

The second bracketed term is the formula for the Fourier coefficient in the sine-sine series expansion for $\partial^2 w / \partial x^2$, and, referring to equations (A2), it may be replaced by $-a_{mn} (m\pi/a)^2$. As a result, equation (A41) becomes

$$b_{mn} = \frac{16pa}{\pi^3 D} \frac{B_n}{n} - a_{mn} \left(\frac{m\pi}{a} \right)^2 \quad (A42)$$

Analogous operations on the second of equations (A40) give

$$c_{mn} = \frac{16pb}{\pi^3 D} \frac{A_m}{m} - a_{mn} \left(\frac{n\pi}{b} \right)^2 \quad (A43)$$

Thus, the b_{mn} and c_{mn} in equations (A39) are now expressed in terms of quantities which are known once the A_{ij} , A_i and B_j have been computed.

Vertical reaction along the edges.— From page 86 of reference 2 the effective vertical shears along the edges $x=0$ and $y=0$, in units of force per unit length, are

$$(V_x)_{x=0} = -D \left[\frac{\partial^3 w}{\partial x^3} + (2-\nu) \frac{\partial^3 w}{\partial x \partial y^2} \right]_{x=0} \quad (A44)$$

$$(V_y)_{y=0} = -D \left[\frac{\partial^3 w}{\partial y^3} + (2-\nu) \frac{\partial^3 w}{\partial y \partial x^2} \right]_{y=0}$$

Replacing the derivatives by their series expansions (A38) and (A39), and utilizing the relations (A42) and (A43), one obtains

$$(V_x)_{x=0} = 16pa\pi^{-3} \sum_{n=1,3,\dots}^N \sum_{m=1,3,\dots}^M S_{mn} \sin(n\pi y/b) \quad (A45)$$

$$(V_y)_{y=0} = 16pa\pi^{-3} \sum_{m=1,3,\dots}^M \sum_{n=1,3,\dots}^N T_{mn} \sin(m\pi x/a)$$

where

$$S_{mn} = A_{mn} m[m^2 + (2-\nu)n^2\beta^2] - B_n n^{-1} \quad (A46)$$

$$T_{mn} = A_{mn} n\beta[\beta^2 n^2 + (2-\nu)m^2] - A_m (m\beta)^{-1}$$

Computational details.- The above analysis was the basis for computing the n_1 and n_3 data in Figures 5 and 7 for values of K other than 0 and ∞ . Calculations were made for $M = N = 11, 13, 15$ and the results were graphically extrapolated to $M = N = \infty$. This technique could not be used successfully for computing n_2 because of poor convergence, or, perhaps, non-convergence, of the series (A45).

APPENDIX B

SMALL-DEFLECTION ANALYSIS OF A UNIFORMLY LOADED ELASTIC RECTANGULAR PLATE WITH CLAMPED EDGES

Here the energy method is again employed in conjunction with Lagrangian multipliers but with a different double Fourier series, to analyze a uniformly loaded rectangular plate with clamped edges. The main purpose is to obtain data for the $K = \infty$ curve of Figure 6 (which data could not be obtained from the analysis in appendix A because of poor convergence). At the same time, expressions are given for the deflections and the edge bending moments. It will be seen that the data needed for the $K = \infty$ curve of Figure 6 are obtained directly from the values of the Lagrangian multipliers.

Coordinate system and notation.— The same coordinate system is used as in appendix A, and the symbols k , E , ν , D , K and β will have the same definitions as in appendix A.

Series for w .— The following series gives zero normal slope at the edges and the deflection symmetry appropriate to a uniform loading:

$$w(x, y) = \sum_{m=0,2,\dots}^M \sum_{n=0,2,\dots}^N a_{mn} \cos(m\pi x/a) \cos(n\pi y/b) \quad (B1)$$

It is understood that calculations will be made with successively higher values of M and N until convergence has been achieved for all physical quantities of interest.

Constraining relations.— The conditions of zero deflection along the edges requires that the following constraining relations be imposed on the coefficients:

$$\sum_{m=0,2,\dots}^M a_{mn} = 0 \quad (n = 0, 2, 4, \dots, N) \quad (B2)$$

$$\sum_{n=0,2,\dots}^N a_{mn} = 0 \quad (m = 0, 2, 4, \dots, M) \quad (B3)$$

These equations are redundant, inasmuch as summing (B2) over n leads to the same equation as summing (B3) over m . In order to remove this redundancy, we shall replace the first of equations (B2) and the first of equations (B3) by the single equation obtained by summing these two. Thus, the following set of independent constraining relations is obtained to replace (B2) and (B3):

$$2a_{00} + \sum_{n=2,4,\dots}^N a_{0n} + \sum_{m=2,4,\dots}^M a_{m0} = 0 \quad (B4)$$

$$\sum_{m=0,2,\dots}^M a_{mn} = 0 \quad (n = 2, 4, 6, \dots, N) \quad (B5)$$

$$\sum_{n=0,2,\dots}^N a_{mn} = 0 \quad (m = 2, 4, 6, \dots, M) \quad (B6)$$

Strain energy of plate.— Substitution of the series (B1) into the strain energy expression for a rectangular elastic plate undergoing small deflections (p. 342 of ref. 2) gives the following formula for the strain energy V_1 of the plate:

$$V_1 = \frac{\pi D b^3}{8a^3} \sum_{m=0,2,\dots}^M \sum_{n=0,2,\dots}^N (m^2 + n^2 \beta^2)^2 (1 + \delta_{m0} + \delta_{0n}) a_{mn}^2 \quad (B7)$$

where δ_{m0} and δ_{0n} are Kronecker deltas.

Potential energy of the applied load.- With the xy-plane as datum, the potential energy V_3 of the applied load is

$$V_3 = -p \iint w dx dy$$

or, in view of equation (B1),

$$V_3 = -p a_{00} \quad (B8)$$

Minimization of the total potential energy.- The total potential energy (TPE) is defined as

$$TPE = V_1 + V_3 \quad (B9)$$

By the same argument as in appendix A, the correct values of the a_{mn} in the series (B1) are those which minimize expression (B9) while at the same time satisfying the constraining relations (B4) to (B6).

Again we have a "constrained minimization" problem which can be solved by setting up the new function

$$TPE^* = V_1 + V_3 - \gamma(2a_{00} + \sum_{n=2,4,\dots}^N a_{0n} + \sum_{m=2,4,\dots}^M a_{m0}) - \sum_{n=2,4,\dots}^N \alpha_n \left(\sum_{m=0,2,\dots}^M a_{mn} \right) - \sum_{m=2,4,\dots}^M \beta_m \left(\sum_{n=0,2,\dots}^N a_{mn} \right) \quad (B10)$$

where γ , α_n , β_m are Lagrangian multipliers, and making it stationary with respect to the a_{mn} 's, γ , the α_n 's, and the β_m 's via the conditions

$$\partial(TPE^*)/\partial a_{00} = 0 \quad (B11)$$

$$\partial(TPE^*)/\partial a_{10} = 0 \quad (i = 2, 4, 6, \dots, M) \quad (B12)$$

$$\partial(TPE^*)/\partial a_{0j} = 0 \quad (j = 2, 4, 6, \dots, N) \quad (B13)$$

$$\partial(TPE^*)/\partial a_{ij} = 0 \quad (i = 2, 4, \dots, M; j = 2, 4, \dots, N) \quad (B14)$$

$$\partial(\text{TPE}^*)/\partial\gamma = 0 \quad (\text{B15})$$

$$\partial(\text{TPE}^*)/\partial\alpha_j = 0 \quad (j = 2, 4, 6, \dots, N) \quad (\text{B16})$$

$$\partial(\text{TPE}^*)/\partial\beta_i = 0 \quad (i = 2, 4, 6, \dots, M) \quad (\text{B17})$$

The last three of these conditions merely reproduce equations (B4), (B5) and (B6). With the differentiations carried out, the first four conditions read as follows:

$$-pab - 2\gamma = 0 \quad (\text{B18})$$

$$\frac{\pi^4 D}{8ab} \cdot \frac{i^4}{\beta^2} \cdot 4a_{i0} - \gamma - \beta_i = 0 \quad (i = 2, 4, \dots, M) \quad (\text{B19})$$

$$\frac{\pi^4 D}{8ab} \cdot j^4 \beta^2 \cdot 4a_{0j} - \gamma - \alpha_j = 0 \quad (j = 2, 4, \dots, N) \quad (\text{B20})$$

$$\frac{\pi^4 D}{8ab} \left(\frac{i^2}{\beta} + j^2 \beta \right)^2 \cdot 2a_{ij} - \alpha_j - \beta_i = 0 \quad \begin{matrix} (i = 2, 4, \dots, M) \\ (j = 2, 4, \dots, N) \end{matrix} \quad (\text{B21})$$

Equations (B18) through (B21), together with (B4), (B5) and (B6), are a system of simultaneous linear algebraic equations defining the a_{ij} , β_i , α_j and γ .

For later use we now introduce the following dimensionless measures of A_{mn} , β_m and α_n :

$$\left. \begin{aligned} A_{mn} &\equiv \pi^4 D a_{mn} / pa^2 b^2 \\ B_m &\equiv 2\beta_m / pab \\ A_n &\equiv 2\alpha_n / pab \end{aligned} \right\} (\text{B22})$$

Simplification of simultaneous equations. - From (B18)

$$\gamma = -pab/2 \quad (B23)$$

With this result substituted into (B19), (B20) and (B21), the latter become, after minor algebraic manipulation,

$$A_{i0} = \beta^2(B_i - 1)/i^4 \quad (i = 2, 4, \dots, M) \quad (B24)$$

$$A_{0j} = (A_j - 1)/(j^4 \beta^2) \quad (j = 2, 4, \dots, N) \quad (B25)$$

$$A_{ij} = 2(A_j + B_i)\beta^2(i^2 + j^2\beta^2)^{-2} \quad \begin{matrix} (i = 2, 4, \dots, M) \\ (j = 2, 4, \dots, N) \end{matrix} \quad (B26)$$

These can be used to eliminate the a_{mn} in equations (B5) and (B6). Those equations can then be written as follows:

$$A_n = [n^{-4}\beta^{-2} - \sum_{m=2,4,\dots}^M 2B_m\beta^2(m^2 + n^2\beta^2)^{-2}] f_1(n) \quad (B27)$$

$$(n = 2, 4, \dots, N)$$

$$B_m f_2(m) = m^{-4}\beta^2 - \sum_{n=2,4,\dots}^N 2A_n\beta^2(m^2 + n^2\beta^2)^{-2} \quad (B28)$$

$$(m = 2, 4, \dots, M)$$

where

$$f_1(n) \equiv n^{-4}\beta^{-2} + \sum_{m=2,4,\dots}^M 2\beta^2(m^2 + n^2\beta^2)^{-2} \quad (B29)$$

$$f_2(m) \equiv m^{-4}\beta^2 + \sum_{n=2,4,\dots}^N 2\beta^2(m^2 + n^2\beta^2)^{-2}$$

If (B27) is now used to eliminate the A_n in (B28), the latter equations become

$$\sum_{q=2,4,\dots}^M B_q c_{mq} = r_m \quad (m = 2, 4, \dots, M) \quad (B30)$$

where

$$c_{mq} \equiv f_2(m) \delta_{qm} - \sum_{n=2,4,\dots}^N 4\beta^4 (m^2 + n^2 \beta^2)^{-2} (q^2 + n^2 \beta^2)^{-2} [f_1(n)]^{-1} \quad (B31)$$

$$r_m \equiv m^{-4} \beta^2 - \sum_{n=2,4,\dots}^N 2n^{-4} (m^2 + n^2 \beta^2)^{-2} [f_1(n)]^{-1}$$

On the basis of these developments we now have the following calculation procedure: Solve equations (B30) (whose number depends only on M) simultaneously for the B_q . With these known, equations (B27) will furnish the values of the A_n . Then equations (B24) to (B26) will yield all the A_{ij} except A_{00} . The latter is defined by equation (B4) as

$$A_{00} = \frac{1}{2} \left[\sum_{n=2,4,\dots}^N A_{0n} + \sum_{m=2,4,\dots}^M A_{m0} \right] \quad (B32)$$

Deflections and edge bending moments.— Once the A_{ij} are known, the deflections and edge bending moments are readily computed. Equation (B1) gives the former as

$$w(x, y) = \frac{pa^4}{D} \cdot \frac{1}{\pi^4 \beta^2} \cdot \sum_{m=0,2,\dots}^M \sum_{n=0,2,\dots}^N A_{mn} \cos \frac{m\pi x}{a} \cos \frac{n\pi y}{b} \quad (B33)$$

The bending moments normal to the edge $x = 0$ are also obtained with the aid of equation (B1) as follows:

$$(M_x)_{x=0} = -D(\partial^2 w / \partial x^2)_{x=0} = pb^2 \pi^{-2} \sum_{n=0,2,\dots}^N \sum_{m=2,4,\dots}^M A_{mn} m^2 \cos(n\pi y/b) \quad (B34)$$

Those along the edge $y = 0$ are obtained in a similar way:

$$(M_y)_{y=0} = -D(\partial^2 w / \partial y^2)_{y=0} = pa^2 \pi^{-2} \sum_{m=0,2,\dots}^M \sum_{n=2,4,\dots}^N A_{mn} n^2 \cos(m\pi x/a) \quad (B35)$$

Vertical reactions along the edges.— The unknown vertical reactions (force per unit of length) along the edges $x = 0$ and $y = 0$ will be sought in the following Fourier series form:

$$(V_x)_{x=0} = pa \sum_{n=0,2,\dots}^N S_n \cos(n\pi y/b) \quad (B36)$$

$$(V_y)_{y=0} = pb \sum_{m=0,2,\dots}^M T_m \cos(m\pi x/a)$$

where the coefficients S_n and T_m are as yet unknown except for the fact that overall equilibrium of the plate requires that

$$pab = 2pa(S_0 b) + 2pb(T_0 a)$$

from which it follows that

$$S_0 + T_0 = 1/2 \quad (B37)$$

In order to determine the S_n and T_m we shall postulate an auxiliary problem, that of a uniformly loaded plate, with edges constrained to have zero normal slope, with prescribed vertical loadings, in the form of (B36), along the edges $x = 0$, $y = 0$, and with the loadings along the other two edges dictated by symmetry. We shall determine the deflection shape $w(x,y)$ for this plate by means of the energy method. and then ask what the prescribed vertical loadings along the edges have to be in

order to reduce the edge deflections to zero, i.e., to bring the plate of the auxiliary problem into the same state of deformation as the plate of the original problem.

To solve the auxiliary problem, we shall again assume the deflections in the form of the series (B1), which again leads to equation (B7) for the strain energy V_1 . The potential energy of the applied loads must now include the potential energy of the prescribed vertical loadings along the edges. Thus, in addition to (B8), we have the following contribution to this energy:

$$V_4 = 2 \int_0^a (V_y)_{y=0} w(x,0) dx + 2 \int_0^b (V_x)_{x=0} w(0,y) dy \quad (B38)$$

Substitution of the series expansions (B36) and (B1) converts this to

$$V_4 = 2pab \sum_{m=0,2,\dots}^M \sum_{n=0,2,\dots}^N a_{mn} \left(\frac{T_m}{2-\delta_{m0}} + \frac{S_n}{2-\delta_{n0}} \right) \quad (B39)$$

The total potential energy (TPE) can now be written as

$$\text{TPE} = V_1 + V_3 + V_4 \quad (B40)$$

where the three terms on the right are defined by equations (B7), (B8) and (B39), respectively.

To find the deflection shape under the given loading, we now make the TPE stationary with respect to the a_{ij} via the equations.

$$\left. \begin{aligned} \partial(\text{TPE})/\partial a_{00} &= 0 \\ \partial(\text{TPE})/\partial a_{10} &= 0 \quad (i = 2, 4, \dots, M) \end{aligned} \right\} \quad (B41)$$

(Cont'd on next pg.)

$$\partial(TPE)/\partial a_{0j} = 0 \quad (j = 2, 4, \dots, N)$$

$$\partial(TPE)/\partial a_{ij} = 0 \quad (i = 2, 4, \dots, M; j = 2, 4, \dots, N)$$

With the differentiations carried out, these become

$$-pab + 2pabT_0 + 2pabS_0 = 0 \quad (B42)$$

$$\frac{\pi D}{8ab} \cdot \frac{1}{\beta^2} \cdot 4a_{i0} + pabT_1 + 2pabS_0 = 0 \quad (i = 2, 4, \dots, M) \quad (B43)$$

$$\frac{\pi D}{8ab} \cdot j^4 \beta^2 \cdot 4a_{0j} + 2pabT_0 + pabS_j = 0 \quad (j = 2, 4, \dots, N) \quad (B44)$$

$$\frac{\pi D}{8ab} \cdot \left(\frac{1}{\beta} + j^2 \beta \right)^2 \cdot 2a_{ij} + pabT_1 + pabS_j = 0 \quad \begin{matrix} i = 2, 4, \dots, M \\ j = 2, 4, \dots, N \end{matrix} \quad (B45)$$

At this point the similarity between this group of equations and equations (B18) to (B21) should be noted.

We now postulate that the loading functions $(V_x)_{x=0}$ and $(V_y)_{y=0}$ are not arbitrary, but are whatever is necessary to give zero deflection along the edges. In that case the plate deflections of the auxiliary problem must be identical with those of the original problem. That is, the a_{ij} in equations (B42) to (B45) will be the same as the a_{ij} in equations (B18) to (B21). It then follows that

$$\begin{aligned}
2pab(T_0+S_0) &= -2\gamma \\
pab(T_1+2S_0) &= -(\gamma+\beta_1) \\
pab(2T_0+S_j) &= -(\gamma+\alpha_j) \\
pab(T_1+S_j) &= -(\alpha_j+\beta_1)
\end{aligned}
\tag{B46}$$

Substituting $\gamma = -pab/2$ (from eq. (B23)), dividing through by $pab/2$, and making use of the definitions (B22), we can convert these equations to the following form:

$$4(T_0+S_0) = 2 \tag{B47}$$

$$2(T_1+2S_0) = 1 - B_1 \tag{B48}$$

$$2(2T_0+S_j) = 1 - A_j \tag{B49}$$

$$2(T_1+S_j) = -(A_j+B_1) \tag{B50}$$

where $i = 2, 4, \dots, M$ and $j = 2, 4, \dots, N$. The first of these equations confirms the equilibrium condition, (B37); and the fourth equation is implied by the first three.

We thus have arrived at the following relationships between the Fourier coefficients in equations (B36) and the dimensionless Lagrangian multipliers A_j and B_i defined by equations (B30) and (B27):

$$S_0 + T_0 = 1/2 \tag{B51}$$

$$T_1 = \frac{1}{2}(1-B_1-4S_0) \quad (i = 2, 4, \dots, M) \tag{B52}$$

$$S_j = \frac{1}{2}(1-A_j-4T_0) \quad (j = 2, 4, \dots, N) \tag{B53}$$

We see that the T_i and S_j have been determined to within a single undetermined constant, say S_0 . The removal of this indeterminacy is discussed in the next section.

Removal of indeterminacy. - We note first that the choice of a value for S_0 can in no way affect the deflections, inasmuch as they are completely determined by the A_j and B_i through equations (B24) to (B26), (B32) and (B33). On the other hand, the value chosen for S_0 will affect the T_i and S_j (see eqs. (B51) to (B53)) and, therefore, the reactions $(V_x)_{x=0}$ and $(V_y)_{y=0}$ (see eqs. (B36)).

The question naturally arises, how can variations in S_0 alter the vertical reactions along the edges (which can just as well be regarded as loads) without at the same time altering the deflections? A plausible conjecture one can make in order to answer this question is that equations (B36) represent not only distributed reactions but also a set of concentrated self-equilibrating forces infinitesimally close to the corners, as shown in Figure 15, and that by varying S_0 we are varying the magnitude of these forces. This conjecture is plausible because concentrated forces such as shown in Figure 15 will alter the mean values of $(V_x)_{x=0}$ and $(V_y)_{y=0}$, and, therefore, S_0 and T_0 , without producing any deflections and without changing the sum $S_0 + T_0$.

Accepting this conjecture, it now becomes clear that S_0 should be so chosen as to cause that component of the reactions represented in Figure 15 to vanish. The reason is that these concentrated forces correspond to Dirac delta function components in $(V_x)_{x=0}$ and $(V_y)_{y=0}$, and if the series (B36) have to represent such components they will not converge in the

usual sense, because their coefficients S_n and T_m will not approach zero as N, M, n and m approach infinity. Thus, if the reaction component shown in Figure 15 is not "swept out" of equations (B36) those equations will be unusable for computing V_x anywhere along the edge $x = 0$ or V_y anywhere along the edge $y = 0$ (not only at the corners).

It has already been mentioned that the presence of any P other than zero in the reactions along the edges will manifest itself through S_n and T_m not approaching zero as N, M, n and m approach infinity. Thus, either of the following conditions should suffice to eliminate any P -forces from equations (B36):

$$\begin{aligned} \lim_{N \rightarrow \infty} S_N &= 0 \\ \lim_{M \rightarrow \infty} T_M &= 0 \end{aligned} \tag{B54}$$

Within the framework of a solution with a finite number of terms, S_N and T_M themselves are the best available estimates of the left-hand sides. Thus, equations (B54) will be replaced by

$$\begin{aligned} S_N &= 0 \\ T_M &= 0 \end{aligned} \tag{B55}$$

and, in view of equations (B52) and (B53), these lead to the following equations for T_0 and S_0 :

$$T_0 = \frac{1}{4}(1 - A_N) \tag{B56}$$

$$S_0 = \frac{1}{4}(1 - B_M) \tag{B57}$$

The following two calculation procedures now suggest themselves:

- (a) Use (B57) to compute S_0 , then (B51) to get T_0 , and accept some degree

of non-satisfaction of (B56). (b) Use both (B56) and (B57) to evaluate T_0 and S_0 and accept some degree of non-satisfaction of (B51). In the second procedure the closeness of $T_0 + S_0$ to $1/2$ can be taken as an overall measure of the convergence. The second procedure is the one that was used in the computations leading to the $K = \infty$ ($\arctan K = \pi/2$) curve of Figure 6.

An alternate hypothesis was also investigated as a basis for removing the indeterminacy in S_0 . This is the hypothesis that at a corner the vertical reaction intensity is continuous around the corner. That is,

$$(V_x)_{x=0,y=0} = (V_y)_{y=0,x=0} \quad (\text{B58})$$

or, in view of (B36),

$$a \sum_{n=0,2,\dots}^N S_n = b \sum_{m=0,2,\dots}^M T_m \quad (\text{B59})$$

Eliminating S_n and T_m through (B52) and (B53), then replacing T_0 by $\frac{1}{2} - S_0$, and then solving for S_0 , one obtains

$$S_0 = \frac{2 + \beta N + M + 2\beta \sum_{n=2,4,\dots}^N A_n - 2 \sum_{m=2,4,\dots}^M B_m}{4(1+N)(1+\beta)} \quad (\text{B60})$$

as the equation defining S_0 on the basis of this second hypothesis. The alternate procedure just described for removing the indeterminacy in S_0 leads to essentially the same numerical results as the first procedure.

APPENDIX C

REMARKS ON THE CORNER STRESS

The analysis of appendix A, which produced the values of R given in Figure 7, is based on the assumption that the rotational spring stiffness k (see eq. (1)) furnished by a wall to the adjacent edge of the lid is constant all along the length of that edge. Since each wall is essentially a wide beam this is a plausible assumption everywhere except near the corners. Where two walls meet at a corner their continuity with each other tends to increase the rotational stiffness of each; in fact, this stiffness approaches infinity right at the corner. This discrepancy between the actual nature of the rotational restraint and that assumed in the analysis is purely a local one. As long as the height h of the package is small compared to the dimensions a and b there should be very little error in any computed quantities except for the corner force R . R is proportional to the rate of twist of the lid at the corner and that, in turn, is strongly dependent on the local constraint conditions at the corner. Consequently, it is highly probable that the R values furnished by Figure 7 are not valid (probably too high) when applied to the lid of a flat-pack under external pressure.

Other considerations lead to the conclusion that the corner reactions for the flat-pack lid might even be zero: If one assumes perfect joint rigidity at the corner, not only between the two walls but also between each wall and the lid, it then follows, by a not too difficult argument, that the rate of twist of the lid must vanish at the corner.* Consequently,

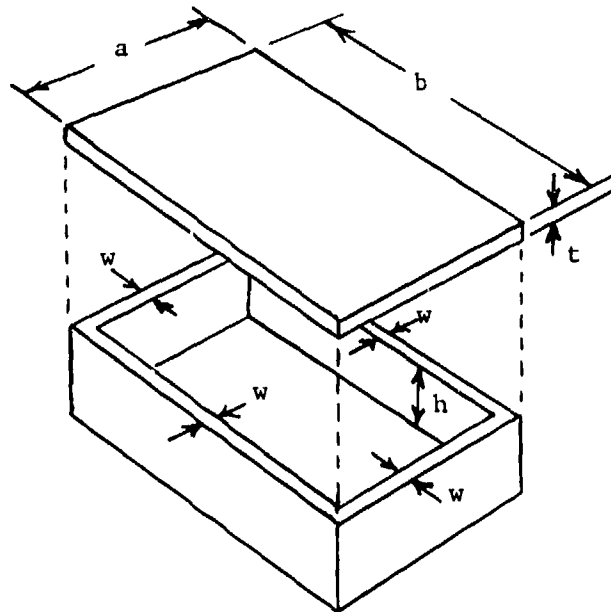
*Referring to Figure 13, consider three points A, B and C infinitesimally close to the corner O. Assume perfect joint rigidity, which implies that right angles are maintained at points 1, 2 and 3 between the pair of dotted lines meeting at each of these points. Now suppose there is some twist of the lid at the corner. This twist will cause point A to move vertically, say downward. The maintenance of right angles at points 1 and 2 will then require that points B and C both move outward. However, this would destroy the right angle which must exist at point 3 between lines C3 and B3. We must, therefore, conclude that point A can have no vertical movement; i.e., the lid can have no twist at the corner.

R , which is proportional to the rate of twist at the corner, must vanish.

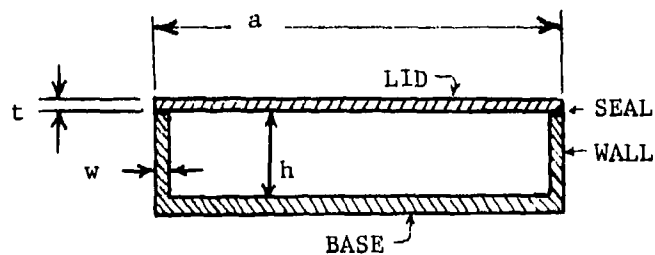
We are thus faced with an uncertainty regarding the magnitude or even the existence of the tensile stress in the seal at the corners of the package. Fortunately, for most packages the proportions are such that S_{edge} , as given by equation (12), will exceed S_{corner} , as given by equation (19). For those packages S_{corner} will not govern in either the design or the screening process, and the question as to whether it exists or whether equation (12) over-estimates it becomes academic. For those rare cases in which S_{corner} , as given by equation (19), might govern, a conservative approach to this question has been outlined in the body of this report.

REFERENCES

1. "Test Methods and Procedures for Microelectronics". MIL-STD-883, Rome Air Development Center (AFSC), Griffiss Air Force Base, New York, 1968.
2. S. Timoshenko and S. Woinowsky-Krieger: Theory of Plates and Shells Second Edition. McGraw-Hill Book Company, Inc., N.Y., 1959.
3. M.S. Kornishin and F.S. Isanbayeva: Flexible Plates and Panels. Report FTD-HC-23-441-69, Air Force Systems Command, Foreign Technology Division, Jan. 21, 1971, AD 722 302. (Translation of Russian book Gibkiye Plastiny i Paneli, 1968.)
4. "Micropackaging Catalog". Bendix Electrical Components Division.

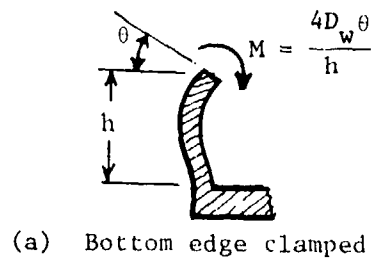


(a) Exploded view

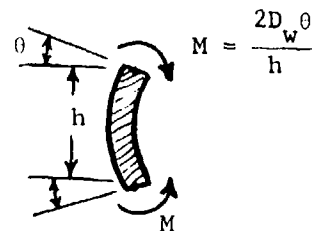


(b) Cross section

Figure 1.- Flat-pack configuration.



(a) Bottom edge clamped



(b) Bottom edge subjected to same moment as upper edge

Figure 2.- Moment-rotation relationships for walls.

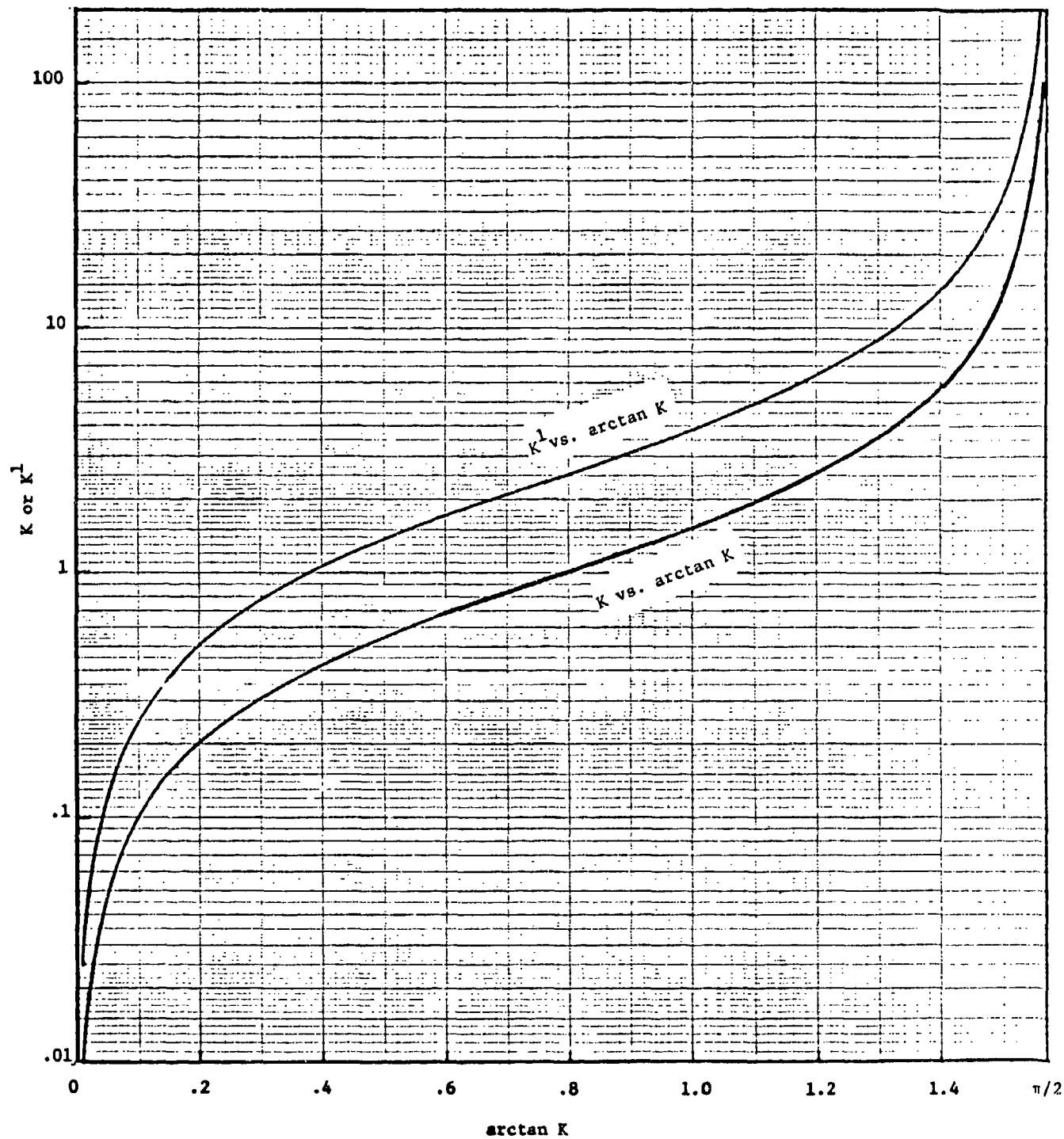


Figure 3.- Relationship between K , K^1 and $\arctan K$.

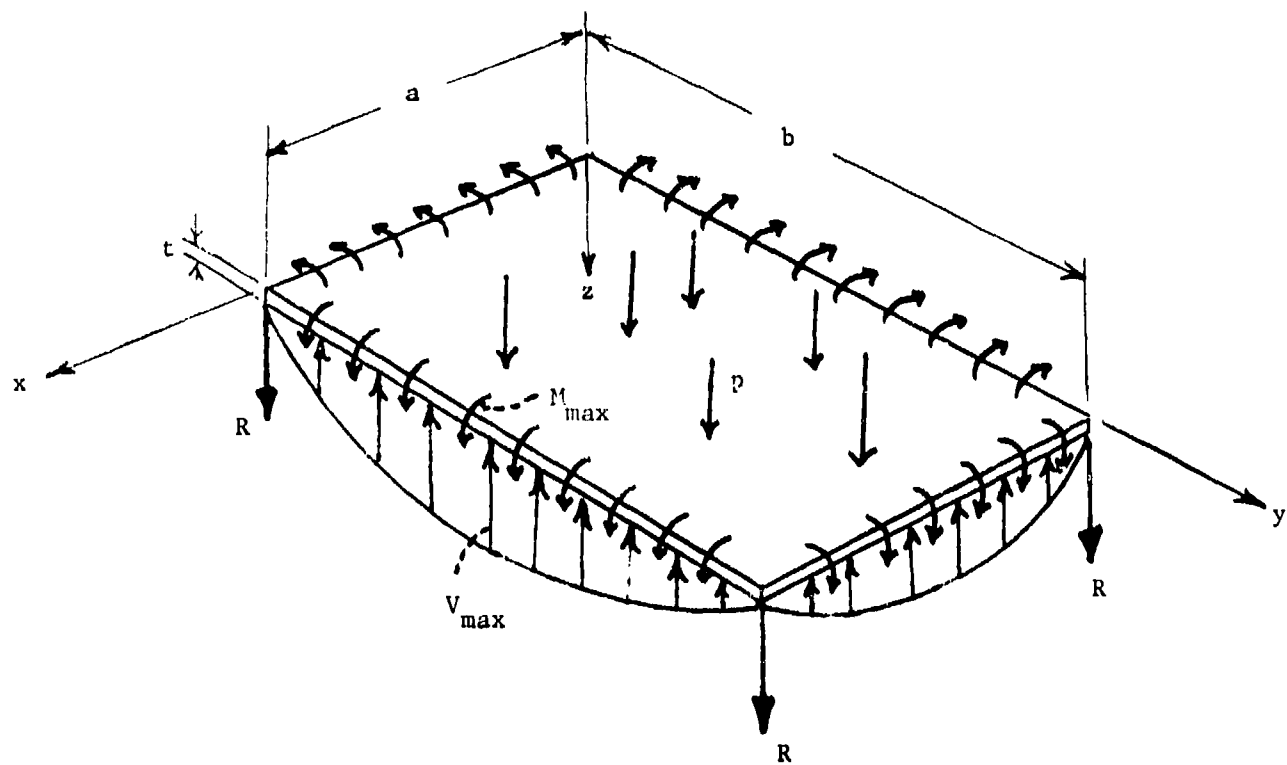


Figure 4.- Reactions at edges and corners of a uniformly loaded rectangular plate with edges elastically restrained against rotation.

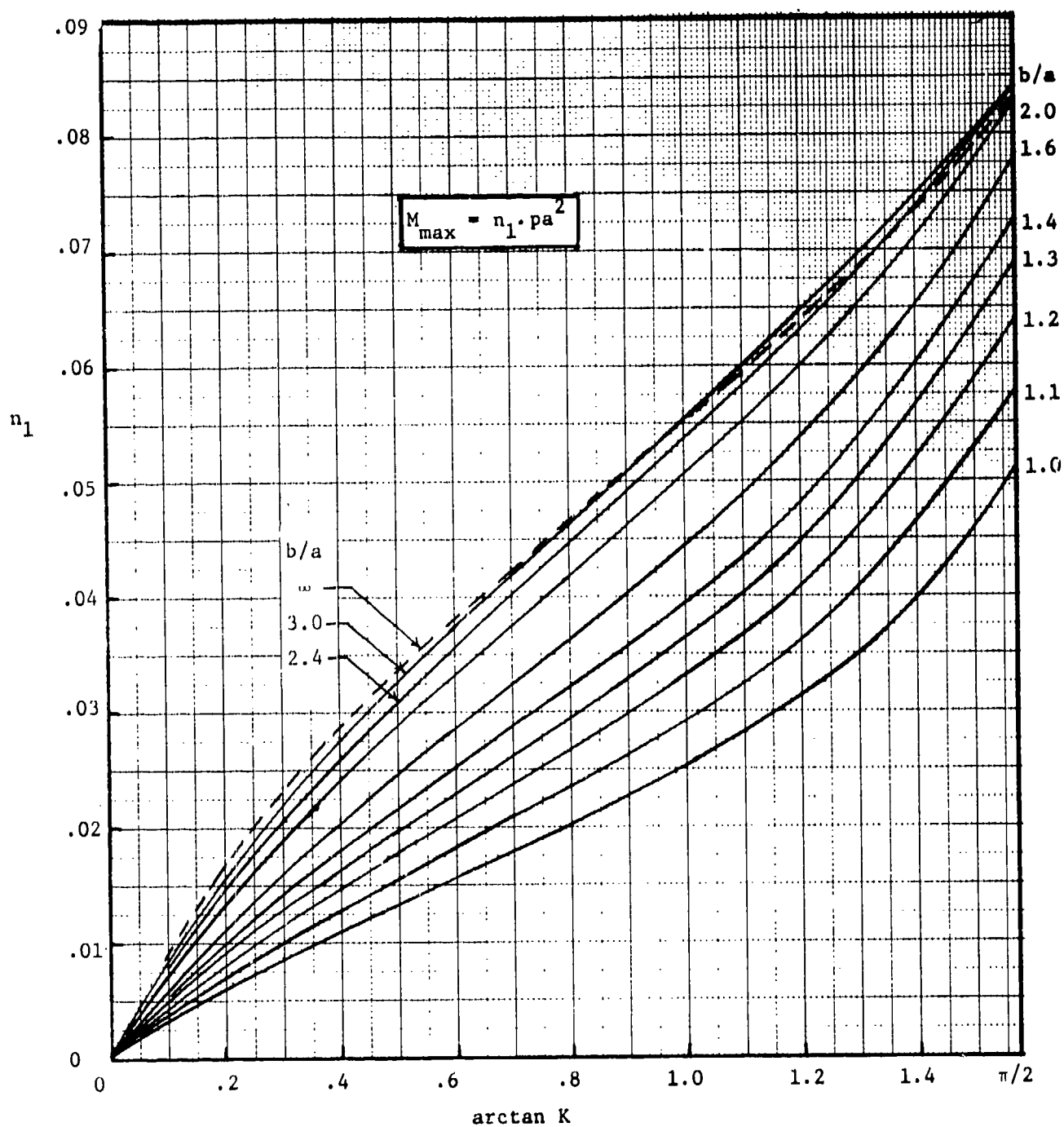


Figure 5.- Bending moment intensity at the middle of the long side for a uniformly loaded rectangular plate with edges elastically restrained against rotation.

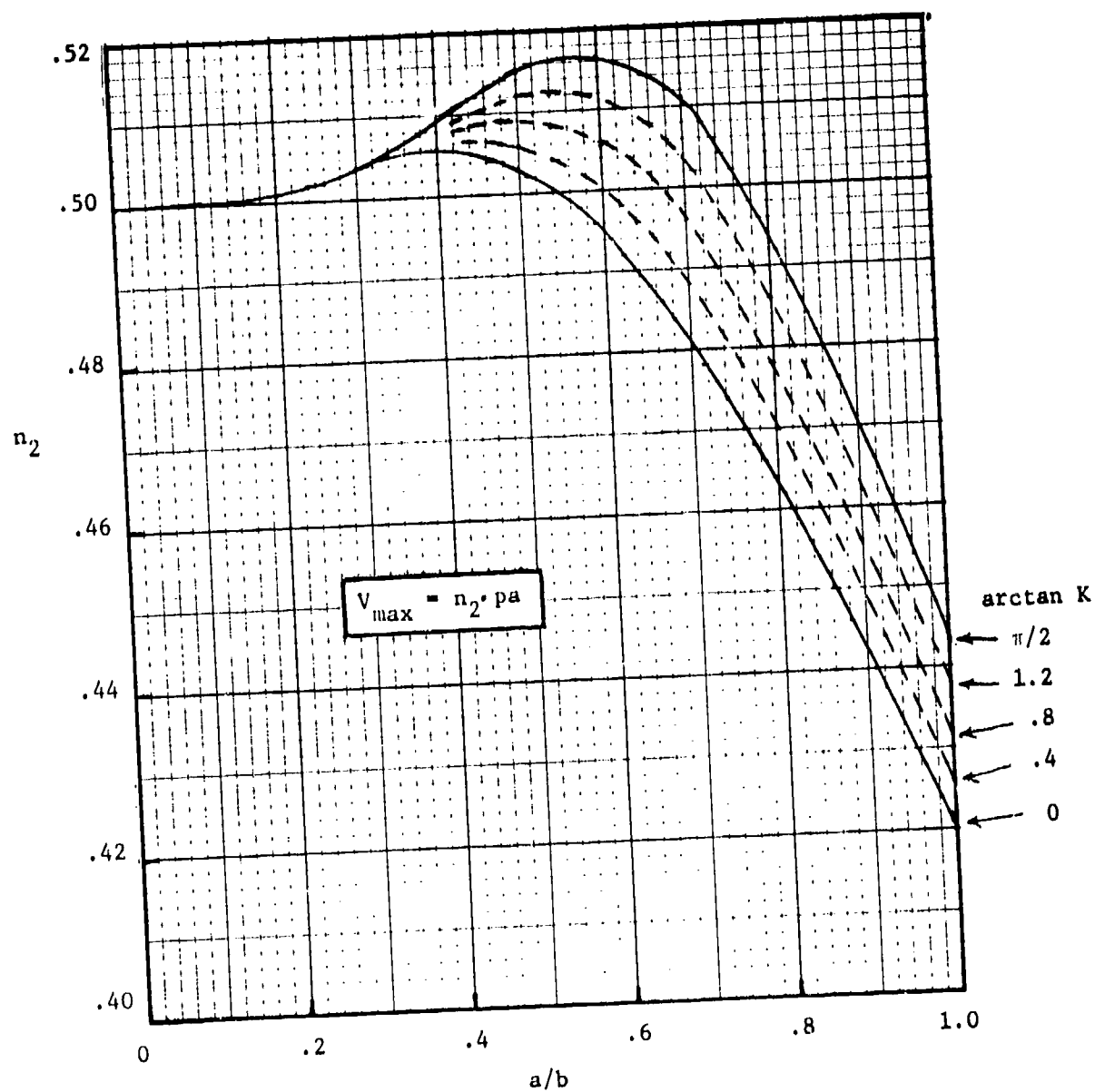


Figure 6.- Intensity of vertical reaction at the middle of the long side for a uniformly loaded rectangular plate with edges elastically restrained against rotation. ($\nu_c = 0.3$)

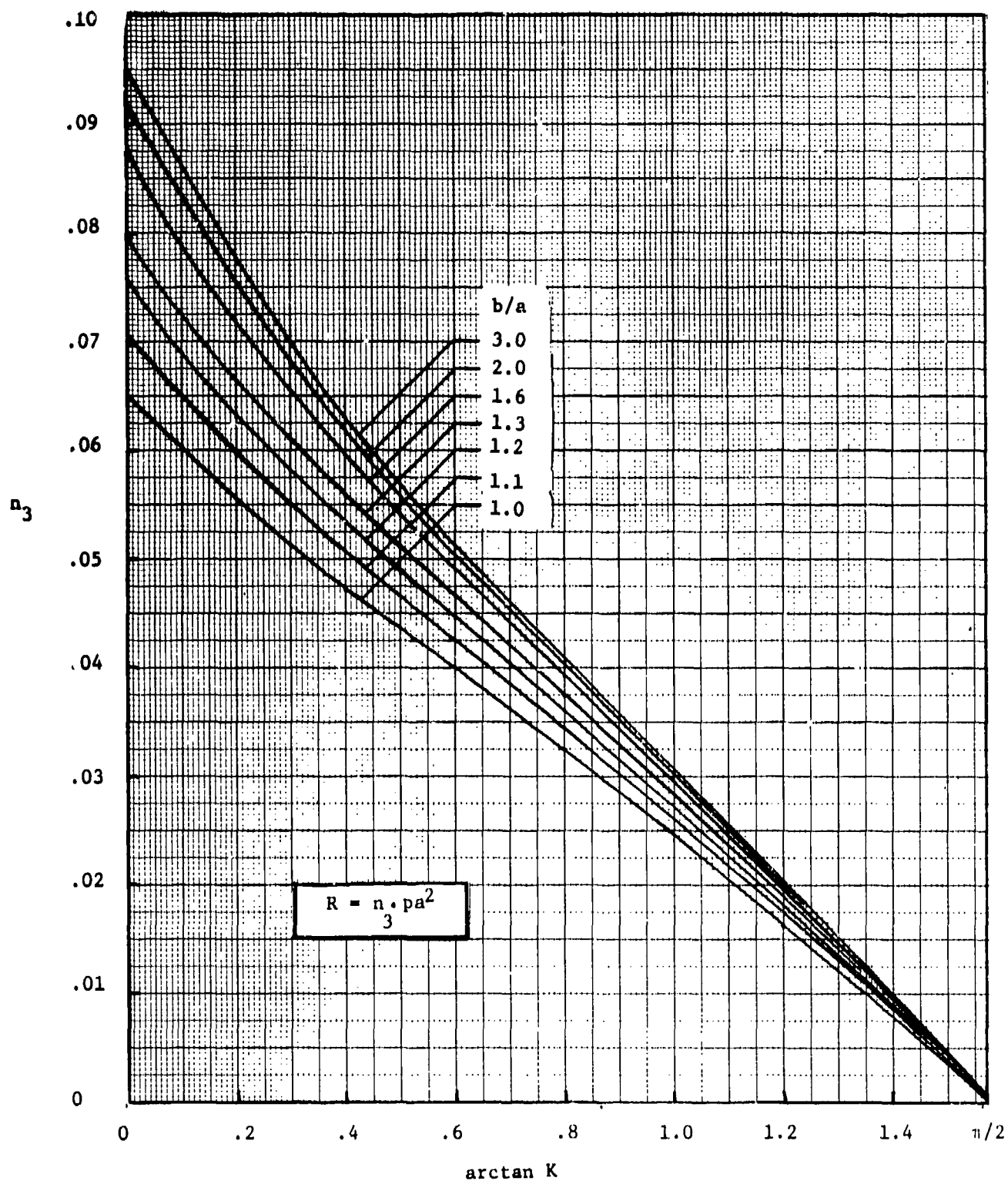


Figure 7.- Magnitude of concentrated corner reaction for a uniformly loaded rectangular plate with edges elastically restrained against rotation. (Applies for $\nu_c = 0.3$. For other values of ν_c multiply ordinate by $(1-\nu_c)/0.7$.)

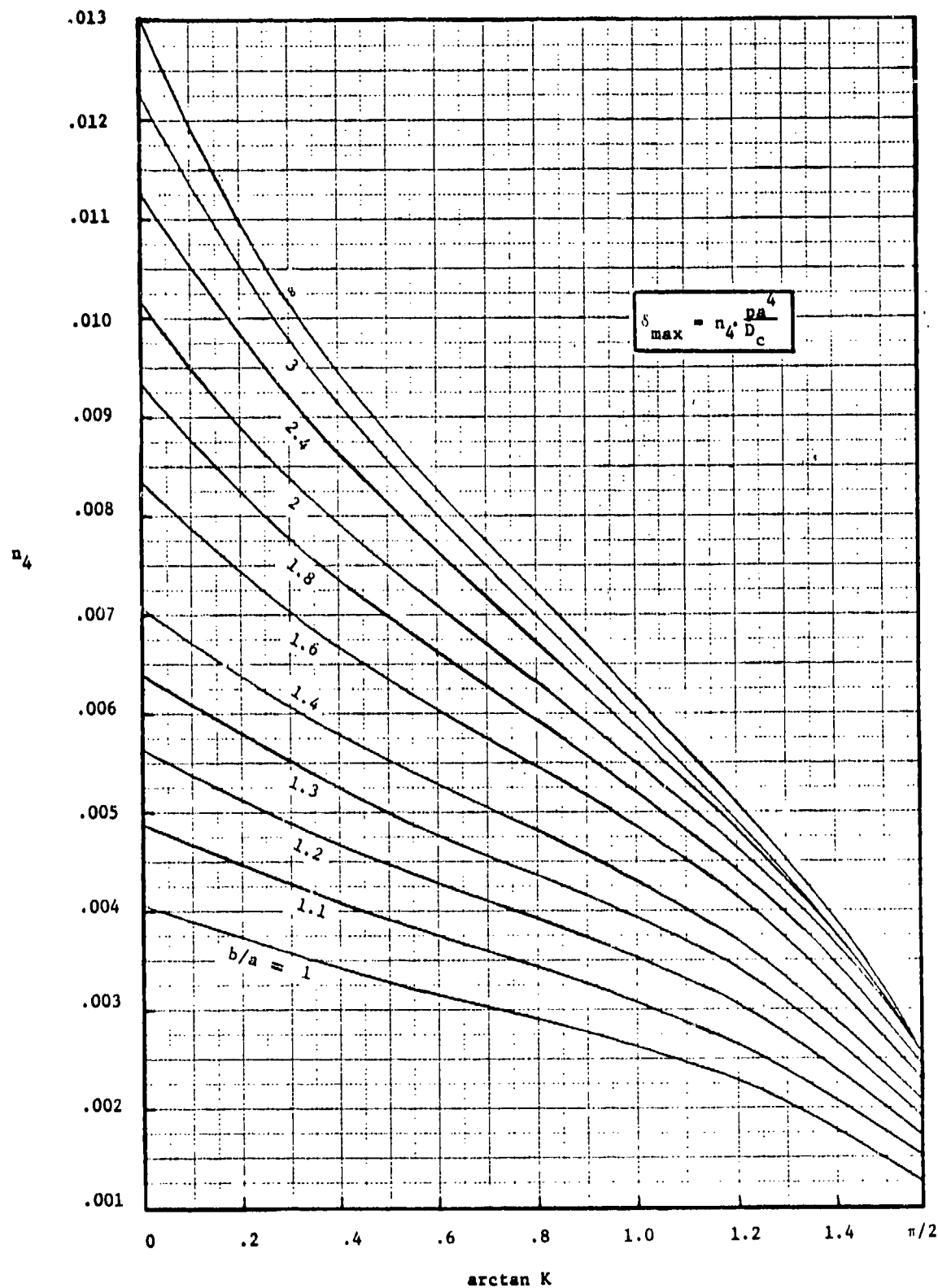


Figure 8.- Center deflection of a uniformly loaded rectangular plate with edges elastically restrained against rotation (small-deflection theory).

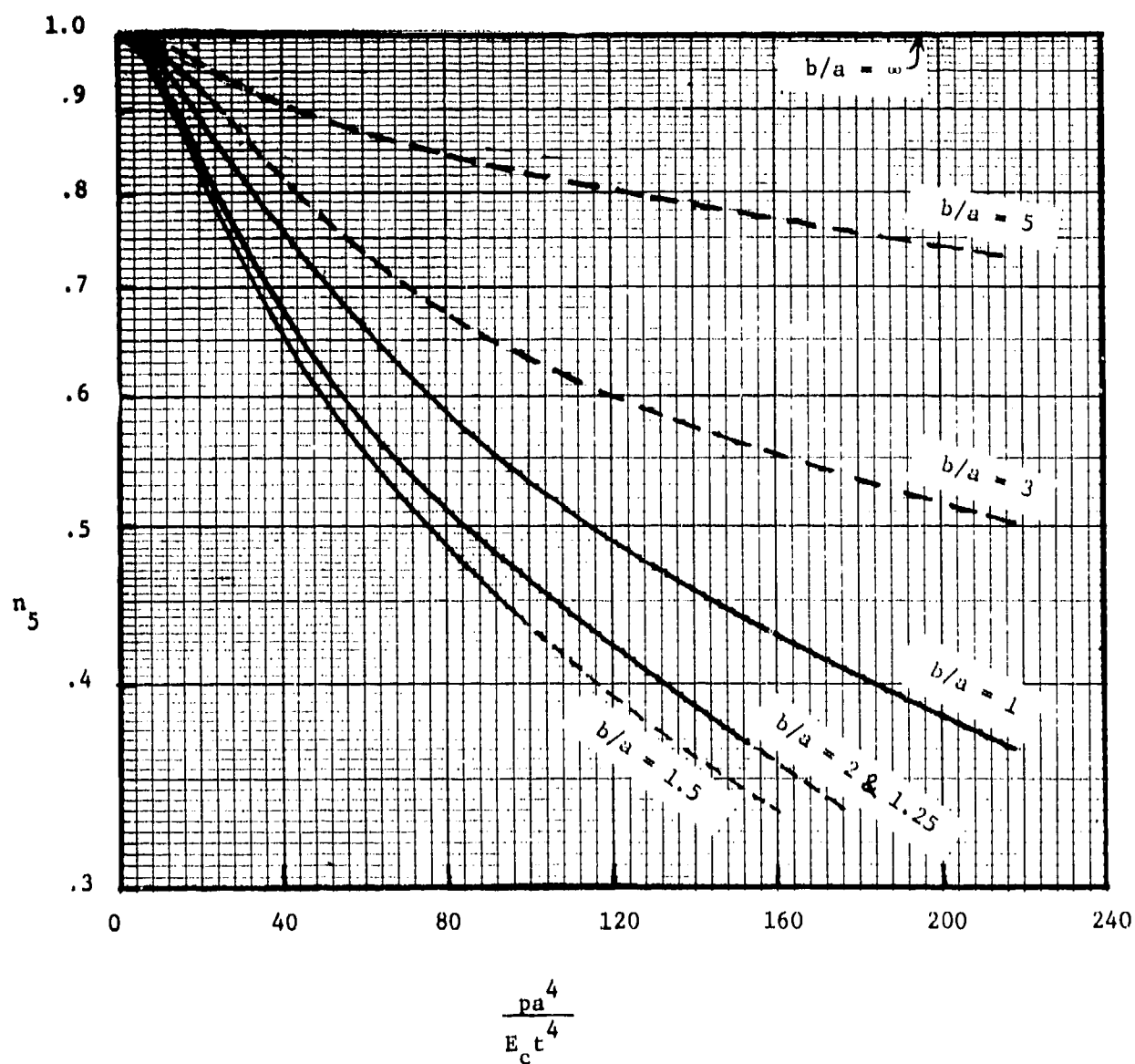


Figure 9.- Correction factor based on large-deflection theory to be applied to the small-deflection-theory value of the center deflection of a flat-pack lid under external pressure ($\nu_c = 0.3$).

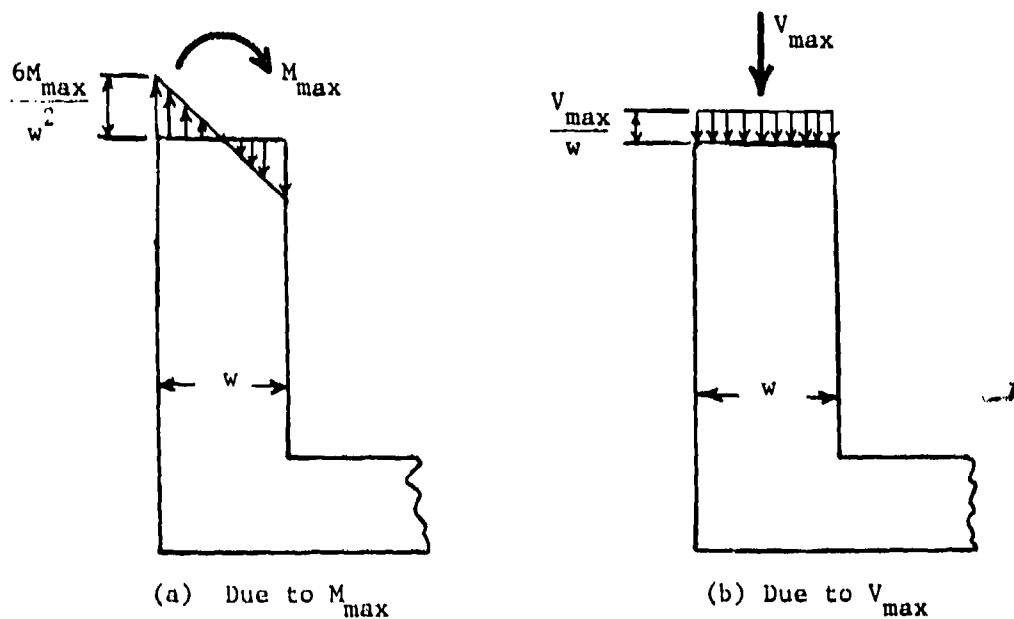


Figure 10.- Stress distributions across the width of the seal at the middle of the long side.

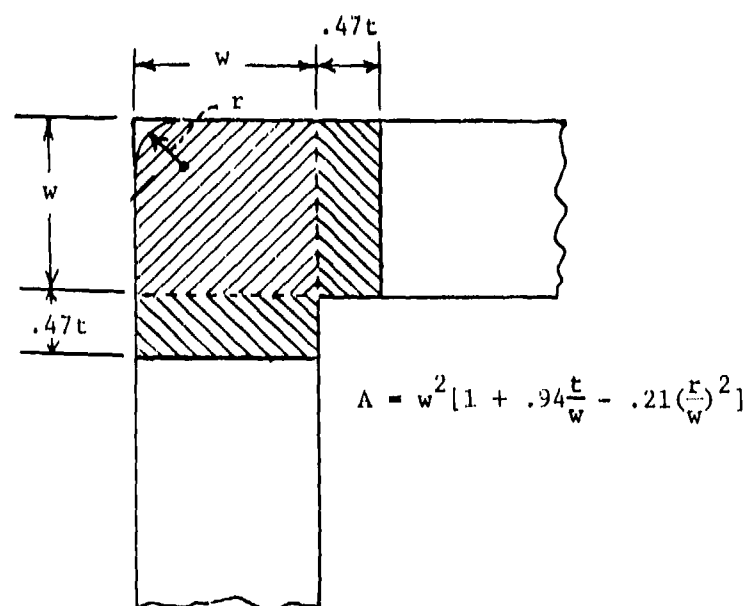


Figure 11.- Area (shaded) over which the corner reaction R is assumed to be distributed.

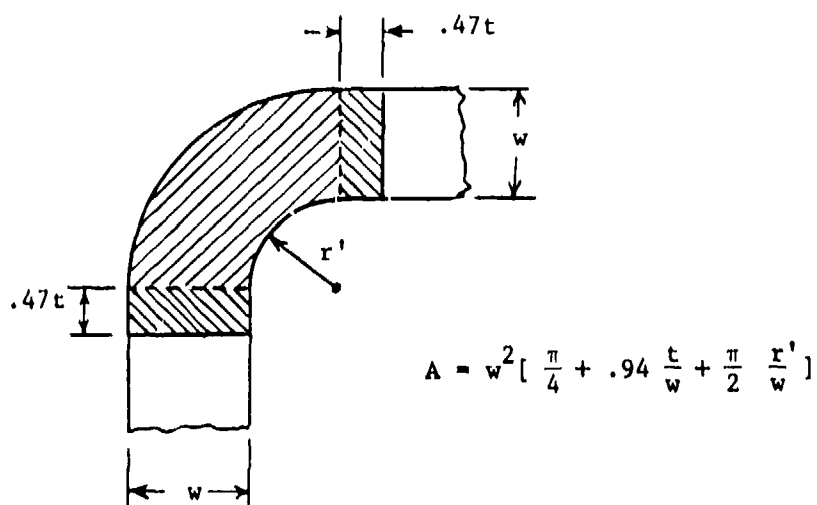


Figure 12.- Area (shaded) over which corner reaction R is assumed to be distributed for package with rounded corners where the walls meet.

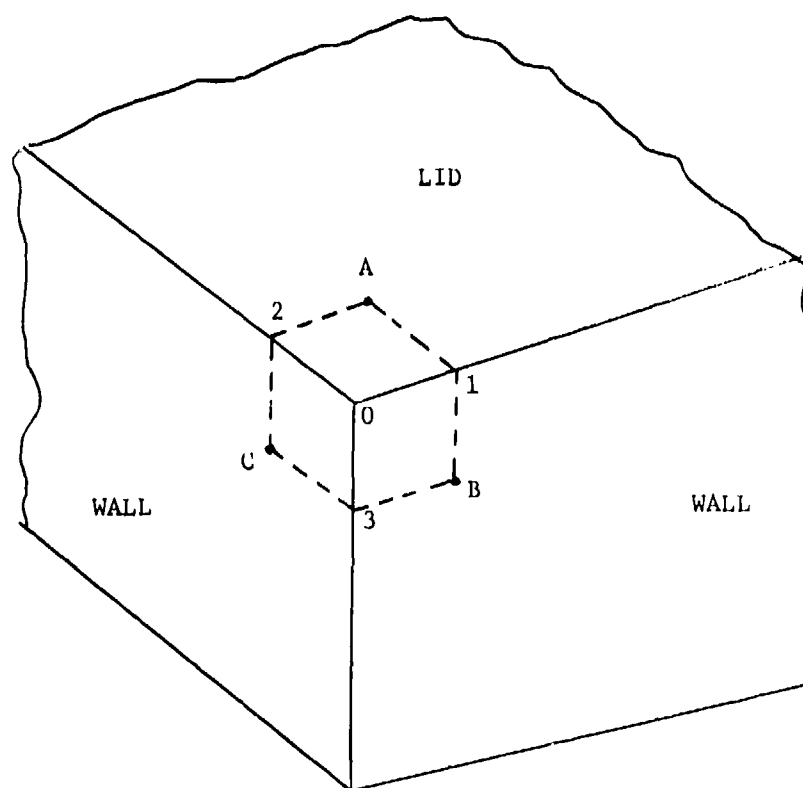


Figure 13.- Points near the junction of two walls and the lid.

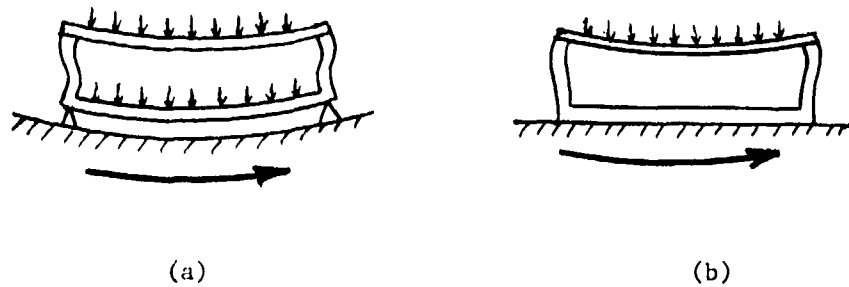


Figure 14.- Two possible kinds of lid-wall-base interaction for a package in a centrifuge.

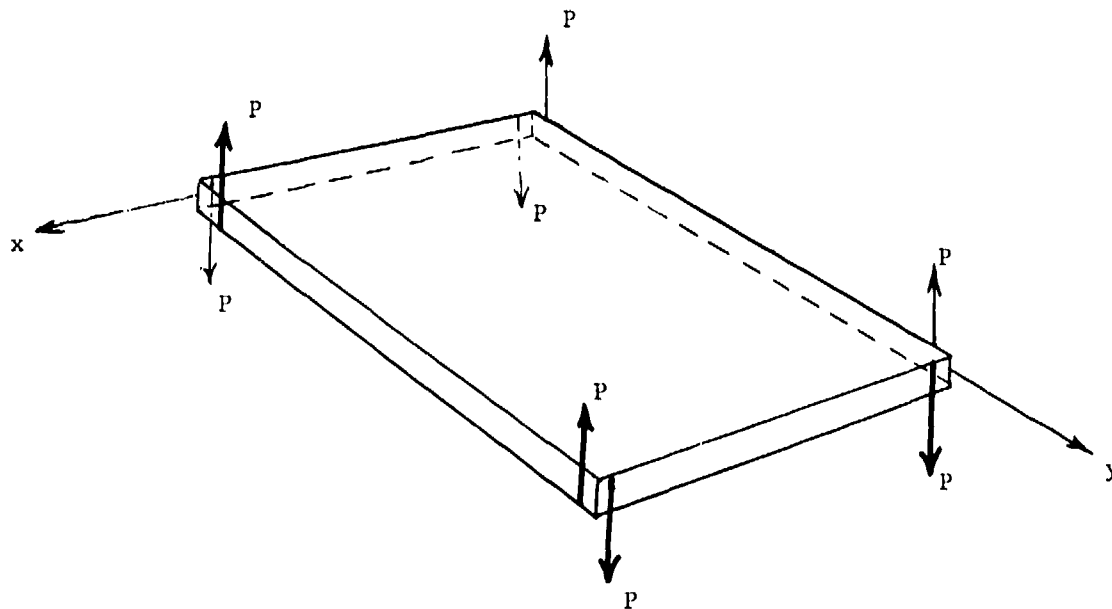


Figure 15.- A loading which will not produce deflections but will alter the Fourier series for $(V_x)_{x=0}$ and $(V_y)_{y=0}$.

MISSION of Rome Air Development Center

RADC is the principal AFSC organization charged with planning and executing the USAF exploratory and advanced development programs for information sciences, intelligence, command, control and communications technology, products and services oriented to the needs of the USAF. Primary RADC mission areas are communications, electromagnetic guidance and control, surveillance of ground and aerospace objects, intelligence data collection and handling, information system technology, and electronic reliability, maintainability and compatibility. RADC has mission responsibility as assigned by AFSC for demonstration and acquisition of selected subsystems and systems in the intelligence, mapping, charting, command, control and communications areas.

